BANK OF CANADA
BANQUE DU CANADA

Staff Working Paper/Document de travail du personnel 2016-61

What Fed Funds Futures Tell Us About Monetary Policy Uncertainty

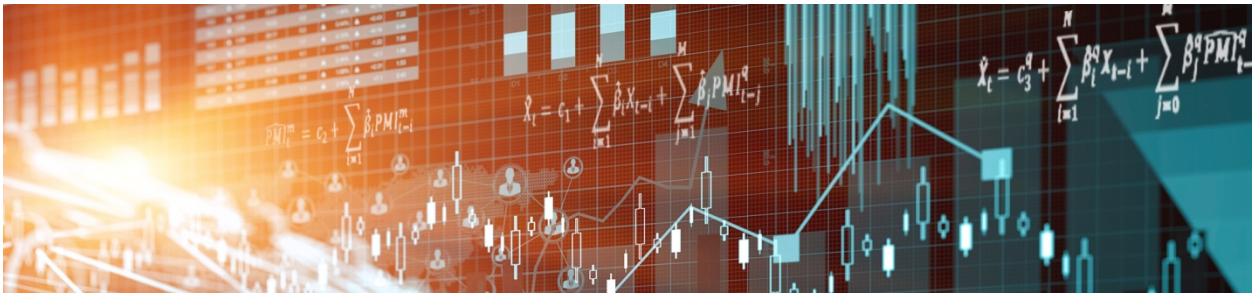

by Jean-Sébastien Fontaine

Bank of Canada Staff Working Paper 2016-61

December 2016

What the Fed Funds Futures Tell Us About Monetary Policy Uncertainty

by

Jean-Sébastien Fontaine

Financial Markets Department
Bank of Canada
Ottawa, Ontario, Canada K1A 0G9
jsfontaine@bankofcanada.ca

ISSN 1701-9397

Acknowledgements

I thank René Garcia, Monika Piazzesi, Jean Boivin, Antonio Diez de los Rios, Bruno Feunou, Itay Goldstein, Sylvain Leduc, Zhongfang He and seminar participants at the Banco de España–Bank of Canada Workshop on Advances in Fixed Income Modeling, HEC Montréal, and the Computational and Financial Econometrics conference for their comments and suggestions. This research was supported by scholarships from the Institut de Finance Mathématique de Montréal and the Banque Laurentienne. An earlier version of the paper was circulated as “Fed Funds Futures and the Federal Reserve.”

Abstract

The uncertainty around future changes to the Federal Reserve target rate varies over time. In our results, the main driver of uncertainty is a “path” factor signaling information about future policy actions, which is filtered from federal funds futures data. The uncertainty is highest when it signals a loosening cycle. The uncertainty raises the risk premium in a loosening cycle, reducing the transmission of target changes to longer maturities. Our results trace the information content of federal funds futures to hedging demand.

Bank topics: Asset pricing; Financial markets; Interest rates
JEL codes: E43; E44; E47; G12; G13

Résumé

L’incertitude entourant les changements à venir du taux cible de la Réserve fédérale évolue dans le temps. D’après les résultats, le principal facteur en cause est la « trajectoire» qui se dégage des contrats à terme sur les fonds fédéraux et qui renseigne sur les actions futures de l’autorité monétaire. L’incertitude est la plus élevée lorsque la trajectoire annonce un cycle d’assouplissement. L’incertitude fait augmenter la prime de risque lors d’un cycle d’assouplissement et atténue la transmission des changements du taux cible aux contrats de plus long terme. Les résultats donnent à penser que les informations contenues dans les contrats à terme sur les fonds fédéraux proviennent des opérations de couverture.

Sujets de la Banque : Évaluation des actifs; Marchés financiers; Taux d’intérêt
Codes JEL : E43, E44, E47, G12, G13

Non-Technical Summary

Federal Reserve communications—statements and speeches—interact with economic conditions to shape the anticipation of investors in the federal funds futures market. Investors anticipate the path of future policy decisions as well as uncertainty surrounding future decisions. This paper measures uncertainty about the future path of policy that investors incorporate into futures prices. The results show that the uncertainty with respect to this path varies through expansions and recessions. In a sample between 1994 and 2017, this uncertainty is lowest when the Federal Reserve is expected to tighten its policy rate and highest when it is expected to loosen its policy rate. Since policy surprises represent a risk to investors, the compensation for risk implicit in federal funds futures decreases because of the lower uncertainty when the Fed is expected to tighten policy. The results are consistent with evidence that forward guidance by the Fed reduced uncertainty when it was tightening its policy rate. This suggests that communication by the Federal Reserve affects both the anticipated path and the uncertainty regarding future policy decisions.

Introduction

Policy decisions by the Federal Reserve regarding the overnight target rate influence expectations about future decisions. However, little is known about the effects these decisions have on the uncertainty surrounding future decisions. This paper sheds some light on this uncertainty and on the response of the risk premium as the Fed manoeuvers the business cycles. This response is important because both expectations and uncertainty can move longer-term interest rates—but not necessarily in the same direction. The response of the risk premium may affect the transmission of policy decisions throughout financial markets.

Measuring the uncertainty around future policy decisions also sheds some light on the apparent gradualism in monetary policy.[1] Gradualism has been interpreted as the endogenous policy response of a central bank that does not want to "spook" the bond market (e.g., Stein and Sunderam, 2015), but the apparent gradualism has also been interpreted as a sequence of exogenous and unpredictable shocks that appear serially correlated after the fact (e.g., Rudebusch, 2002). These mechanisms for gradualism have different implications for the correlation between expectations and uncertainty.

Conceptually, the approach in this paper exploits the well-established information content of federal funds futures. Indeed, the most common way to identify policy surprises uses the change of federal funds futures rates following Federal Open Market Committee (FOMC) meetings (e.g., Cochrane and Piazzesi, 2002; Bernanke and Kuttner, 2005). These futures are also widely used to measure expectations about future policy decisions (Krueger and Kuttner, 1996). But these futures can also provide information about the uncertainty surrounding future decisions. This paper combines daily federal funds futures data with a dynamic term structure model (DTSM) to identify the expectations and the distribution of future policy decisions. This approach offers three main empirical contributions.[2]

[1] The benefits and rationale of forward-guidance and gradualism near the lower bound are well-understood; see e.g., Krugman (1998); Eggertsson and Woodford (2003).

[2] Federal funds futures are short-term financial contracts linked to the overnight federal funds rate, which

First, regarding the uncertainty about future decisions, we provide new evidence on the distribution of possible changes to the target rate. The dispersion of this distribution, measured by its volatility, is our proxy for uncertainty. Our findings reveal that the volatility is highly cyclical and varies with the expected "path" of future target rates. This path factor represents expectations about future target rates and is filtered jointly with volatility from federal funds futures. The volatility of changes to the target rate is lowest in anticipation of a higher path for target rates. Conversely, the volatility is highest in anticipation of a lower path for target rates. The shape of the distribution of changes to the target rate also varies. The distribution is skewed toward hikes in a tightening cycle (at a time when volatility is low) but it is almost symmetric in a loosening cycle (at a time when volatility is high).

This new empirical result points out that the anticipations of market participants are more certain when economic conditions indicate that the target rate will be rising. In other words, market participants are more confident about the size and direction of policy changes when the Fed is leaning against inflation risk in an expanding economy than when supporting employment in a slowing economy. This cyclical pattern complements the existing evidence of a downward trend in the uncertainty since the late 1980s (Swanson, 2006).

Second, the risk premium varies with the cyclical volatility of changes to the target rate. The price of target rate risk is negative and significant. In other words, changes to the FOMC target that are higher than expected are associated with states when marginal utility is higher. This may reflect the oft-cited fears that the Fed will increase the target rate too much (when tightening) or that it will not decrease it enough (when loosening). Therefore, assets with payoffs that vary with the target rate are risky. This component of the risk premium due to target rate risk rises mechanically when the target rate volatility increases.

This result emphasizes a different channel through which policy shocks affect interest

is targeted by the Federal Open Market Committee (FOMC). These futures provide accurate forecasts of target rates (Gurkaynak, Sack, and Swanson, 2012). federal funds futures can identify the volatility of future target rates because pricing short-term interest rates amounts to deciding on the probabilities of a few combinations over a handful of future meetings.

rates. The higher variance of policy shocks in the early stages of a loosening cycle raises the risk premium and mutes the transmission of policy decisions to longer interest rates. This channel is distinct from the effect of economic conditions on the risk premium. The model also allows the price of risk associated with economic conditions to vary. In the results, this component of the risk premium increases when the path variable declines.

Regarding gradualism, the endogenous mechanism in Stein and Sunderam (2015) predicts that a gradual path for future target rates is associated with lower uncertainty, irrespective of the direction of this path. The evidence supports this mechanism in expansion but not in recession, where a gradual downward path is associated with higher volatility. Conversely, the exogenous mechanism in Rudebusch (2002) is consistent with the higher volatility in recession. Additional evidence in Cieslak (2016), based on survey data, shows large and correlated forecast errors in the early stages of recession, suggesting that policy decisions were gradual only in appearance. Overall, the evidence supports different causes for gradualism in expansions or in recessions, which may explain why the debate endures.

Piazzesi and Swanson (2008) suggest that the additional information content of federal funds futures is due to hedging demand pressures. Additional results confirm this interpretation. Several diagnostic checks also support the results. Pricing errors are small. Forecasts of the target rates are unbiased and accurate relative to standard benchmarks (Gurkaynak, Sack, and Swanson, 2012). These checks show that the model correctly captures the historical dynamics and the risk premium. The risk premium estimates contrast with results from unrestricted predictive regressions. Predictive regressions over-fit excess returns early in recessions and imply risk premiums that are too large and too volatile—these large excess returns are due to unexpected recessionary shocks (Cieslak, 2016).

The important role played by the path factor throughout the results is consistent with Sack (2004) and Gurkaynak, Sack, and Swanson (2005), showing that the unanticipated component of FOMC statements can be described in terms of a shock to the current target

rate as well as a shock to the path of future policy decisions (see also Swanson, 2016). Estimates from the model reveal the same decomposition between the shocks to the current target and to the path factor. The results show that the path is also the most significant driver of uncertainty around future policy decisions.

The negative correlation between the path and the uncertainty of future target rates complements Cieslak and Povala (2016). They find that short-rate expectations become more volatile than risk premiums before recessions. This paper is distinct because of several features identifying the volatility associated with future policy decisions.[3]

Changes in federal funds futures rates are widely used to measure the effect that unanticipated changes to the target have on longer-term yields (Kuttner, 2001). However, Rigobon and Sack (2004) show that the response of asset prices to policy shocks can also be identified based on the increase in the variance on days of FOMC meetings. The approach in this paper integrates both identification strategies.

Rudebusch (1998) shows that policy shocks obtained from recursive identification of vector autoregression (VAR) residuals has a low correlation with shocks measured from daily futures data. Faust, Swanson, and Wright (2003) show how to use shocks measured from daily futures within VARs. They find that these two identification strategies—recursive identification or using futures data—can have different implications (see also Rogers, Scotti, and Wright, 2016, in the context of international markets). This is essentially the approach taken here: the policy shocks are identified based on the changes in futures rates on days with an FOMC meeting. The difference is that identification occurs within the model and not in a preliminary step. Interestingly, the specification of the target rate in this paper has a VAR representation amenable to implementations in a structural framework.

The model is a discrete-time variant of Piazzesi (2005a). These no-arbitrage term struc-

[3]These are (i) the sample is daily, (ii) the model is adapted to the observed discrete changes to the target rate and (iii) the estimation exploits the information content of futures (instead of yields with more than two years to maturity).

ture models are designed to match the properties of the target rate. The target rate exhibits a step-like path with changes taking only a small number of values and occurring following infrequent FOMC meetings.[4] Piazzesi (2005a) documents significant improvements over standard dynamic term structure models at short maturities. This paper relies on a few key extensions relative to Piazzesi (2005a). First, the price of target rate risk is not restricted to zero and, therefore, the risk premium may vary with the volatility of target rate changes. Second, the volatility of changes to the target rate is not constant. Third, the sample includes data on federal funds futures. There are several classes of DTSMs that generate time-varying volatility in yields, but they do not identify the volatility of policy shocks (Cox et al., 1985; Bansal and Zhou, 2004; Ang et al., 2011).

The analysis covers the period between 1994 and 2008. This choice of sample period consciously ignores several important but confounding issues present in the data since 2008. Interest rates reached a lower bound around zero in the United States. Since then, the compression of volatility due to the lower bound has a dominant role in the data. In addition, the Fed introduced long-term asset purchases and changed its communication of forward guidance in a few instances, complicating the relationship between expectations and uncertainty. The results in a pre-2008 sample are useful since they highlight the relationship between expectation and uncertainty in "normal" times. The conclusion discusses potential extensions of the model to incorporate the effects of the lower bound.

The rest of the paper is organized as follows. Section I details the discrete-time dynamic term structure model. Section II summarizes the data as well as the specification and estimation of the model. Section III documents the cyclical variations of target rate uncertainty, discusses the impact on the risk premium and analyzes the effect of hedging demand on the information content of forward-to-futures spreads. Section IV concludes.

[4]Fontaine (2014) considers a simpler variant that is identical to a benchmark Gaussian term structure model but with discrete target rate changes. Using a Gaussian distribution yields misleading estimates of policy rule coefficients.

I Model

A A Model of Discrete Target Changes

The effective overnight rate r_t^{eff} can be decomposed into the Fed target rate and a spread: $r_t^{eff} = r_t + s_t$.[5] The specification of the effective spread s_t will be discussed in Section C. Target changes can be written as

$$r_{t+1} - r_t = \Delta n_{t+1},$$

where Δ is a 0.25 percent increment and where n_t is distributed over a discrete integer support $n \in \{\ldots, -2, -1, 0, 1, 2, \ldots\}$. Except for a discrete support, this representation is general. In practice, most FOMC meetings result in changes 0 or 1 increment with a few exceptions where the FOMC changes its target by 2 or 3 increments. This suggests a simple representation:

$$r_{t+1} - r_t = \Delta \left(n_{t+1}^u - n_{t+1}^d \right), \tag{1}$$

where $n_{t+1}^u \sim \mathrm{P}(\lambda_{t+1}^u)$ and $n_{t+1}^d \sim \mathrm{P}(\lambda_{t+1}^d)$ are independent random variables with Poisson distribution conditional on time-t information. The u and d superscripts identify n_{t+1}^u and n_{t+1}^d with *up* and *down* Poisson components of the distribution, respectively. The intensity parameters depend on the occurrence of a scheduled FOMC meeting at date $t+1$.[6] If there is a scheduled FOMC meeting, the intensity parameters λ_{t+1}^u and λ_{t+1}^d depend on the state

[5] See Hamilton (1996) for detailed discussions of the overnight federal funds market.

[6] The FOMC schedule is available publicly at least one year in advance. Piazzesi (2005b) discusses jumps with time-varying intensities but with deterministic jump time in continuous time. A discrete-time specification offers tractability gains over a continuous-time specification. First, federal funds futures rates are not affine. Second, the schedule of FOMC meeting is not time homogenous. These complications lead to non-standard and intractable differential equations in continuous time. By contrast, a discrete-time model yields recursions that are easily implemented.

variables X^*_{t+1}:

$$\lambda^u_{t+1} = \lambda + \lambda_u^\top \left(X^*_{t+1} - \bar{X}\right) \text{ and } \lambda^d_{t+1} = \lambda - \lambda_d^\top \left(X^*_{t+1} - \bar{X}\right), \tag{2}$$

where $\bar{X} \equiv E[X^*_t]$. The FOMC may change its target rate following an unscheduled meeting. The intensities for these rare changes are constant λ^u_0 and λ^d_0.[7]

B Properties of the Target Rate

Equation 1 specifies the conditional distribution of target rate changes. Conditional on X^*_{t+1}, the distribution of target rate changes is affine (i.e., its conditional Laplace transform is exponential-affine). Its conditional mean, variance and skewness are given by affine function of the state variables. This follows from existing results for the difference between two independent Poisson processes (see Appendix A.1).

Consider dates where an FOMC meeting is scheduled. In the stationary state $X^*_{t+1} = \bar{X}$ the distribution of a target change is symmetric with mean zero and variance $2\lambda\Delta^2$. Otherwise, the conditional mean, variance and asymmetry depend on the states. The expected target change is given by

$$E[r_{t+1} - r_t | X^*_{t+1}] = \Delta(\lambda_u + \lambda_d)^\top (X^*_{t+1} - \bar{X}). \tag{3}$$

This specification embodies a wide range of policy rules with different state variables or parametric restrictions. Note that λ_u and λ_d cannot be identified separately based on the conditional mean equation only. For instance, these parameters cannot be estimated separately by regressing target rate changes on some state variables. The conditional variance of

[7]Balduzzi, Bertola, and Foresi (1997) and Balduzzi et al. (1997) investigate the implications of discrete target changes for the term structure of interest rates. Johannes (2004) provides conclusive evidence that the persistent policy jumps in the target are the key drivers of other short-term rates. In a forecasting context, Hamilton and Jordà (2002) combine an ordered response function with a conditional hazard rate but do not impose no-arbitrage restrictions (see also Grammig and Kehrle, 2008).

a target rate change is given by

$$Var_t[r_{t+1} - r_t | X^*_{t+1}] = \Delta^2(2\lambda + (\lambda_u - \lambda_d)^\top (X^*_{t+1} - \bar{X})). \tag{4}$$

The variance of a target change is different around scheduled FOMC meetings. Rigobon and Sack (2004) use this feature to identify monetary policy from high-frequency data. In addition, the variance of a target change changes with the state of the economy at FOMC meetings. The conditional mean depends on $\lambda_u + \lambda_d$ but the variance depends on $\lambda_u - \lambda_d$. The conditional variance can be used to identify λ_u and λ_d. In fact, the model could be re-parameterized with $\lambda_u + \lambda_d$ and $\lambda_u - \lambda_d$.

It is useful to see how the difference of two Poisson innovations can generate separate time variations in the mean and variance. Take one element k of the state vector $X^*_{k,t}$ that is positively correlated with the conditional mean: $\lambda_{u,k} + \lambda_{d,k} > 0$. If $\lambda_{u,k} - \lambda_{d,k} < 0$, then the increase in the variance of n^u_{t+1} is smaller than the decrease in the variance of n^d_{t+1} when $X^*_{k,t}$ increases. Since n^u_{t+1} and n^d_{t+1} are (conditionally) independent, the variance of $n^u_{t+1} - n^d_{t+1}$ decreases. In this example, the mean is positively correlated with $X_{k,t}$, but the variance is negatively correlated. The empirical section pays special attention to the cyclical behavior in the variance of FOMC shocks.

Finally, the conditional skewness of target changes is given by

$$Skew[r_{t+1} - r_t | X^*_{t+1}] = (\lambda_u + \lambda_d)^\top (X^*_{t+1} - \bar{X}) / ((2\lambda + (\lambda_u - \lambda_d)^\top (X^*_{t+1} - \bar{X})))^{3/2}. \tag{5}$$

The relationship with X^*_{t+1} is similar to that of the conditional mean whenever $\lambda_u = \lambda_d$. More generally, the relationship is not linear and depends on the magnitude of $\lambda_u + \lambda_d$ relative to $\lambda_u - \lambda_d$.

C State Variables

The following state variables summarize the information set available to the FOMC immediately *before* a policy decision:

$$X_{t+1}^{*} \equiv \left[r_t \; s_{t+1} \; z_{t+1} \; l_{t+1}\right]^{\top}, \tag{6}$$

where z_{t+1} and l_{t+1} represent public macroeconomic or financial information. In contrast, the information set relevant to investors at the end of a day with an FOMC meeting is summarized by

$$X_{t+1} \equiv \left[r_{t+1} \; s_{t+1} \; z_{t+1} \; l_{t+1}\right]^{\top}. \tag{7}$$

The variables r_t and s_t are observed directly. The latent factor z_t and l_t will be filtered from the data.[8]

It will be useful to provide some intuition about the role of z_t and l_t. The state z_t will play the role of a generic latent factor. The results will show that this role is that of a "path" factor capturing the information relevant for future target changes. By contrast, the role of l_t is distinct from z_t by construction because of its role for pricing LIBOR loans. Specifically, the price $D^{l}(t,m)$ of a LIBOR loan with maturity m is given by

$$D^{l}(t,m) \equiv E_t\left[M_{t,t+m} \exp\left(-\sum_{i=0}^{m-1} l_{t+i}\right)\right], \tag{8}$$

for some stochastic discount factor (SDF) M_t. This SDF will be specified in Section E. The reduced-form approach for pricing LIBOR loans in Equation 8 borrows from Grinblatt (2003) and Duffie and Singleton (1997). To interpret the role of l_t, compare with the price of a risk-free loan, $D^{rf}(t,m) \equiv E_t\left[M_{t,t+m}\right]$. It follows, that l_t determines the marginal compensation

[8]This specification implies that the information set of investors corresponds to that of the FOMC at the time of the meeting. In other words, the intra-day variations following the announcement are negligible or can be attributed to information from the FOMC meeting being slowly incorporated into prices. Finally, including s_{t+1} in X_{t+1}^{*} is an abuse of notation, but this is irrelevant for the results.

offered to investors by LIBOR loans, which may be due to a combination of funding risk, default risk or market power. The state l_t is a "spread" factor capturing the information in the cross-section of forward-to-futures spreads.

D Historical Dynamics

The latent path and spread factor z_{t+1} and l_{t+1} follow VAR(1) dynamics,

$$\begin{bmatrix} z_{t+1} \\ l_{t+1} \end{bmatrix} = \begin{bmatrix} \mu_z \\ \mu_l \end{bmatrix} + \begin{bmatrix} \phi_z & \phi_{z,l} \\ \phi_{l,z} & \phi_l \end{bmatrix} \begin{bmatrix} z_t \\ l_t \end{bmatrix} + \begin{bmatrix} \epsilon^z_{t+1} \\ \epsilon^l_{t+1} \end{bmatrix} \tag{9}$$

where ϵ^z_t and ϵ^l_t are i.i.d Gaussian innovations with variance σ^2_z and σ^2_l and covariance σ_{zl}. The effective spread has autoregressive dynamics with order one,

$$s_{t+1} = \mu_s + \phi_s s_t + \epsilon^s_{t+1} + J^s_{t+1}, \tag{10}$$

where $\epsilon^s_t \sim N(0, \sigma^2_s)$ and where J^s_{t+1} follows a compound Poisson distribution with the number of jumps $n^s_{t+1} \sim P(\lambda_s)$ and jump size $\nu^s_{t+1} \sim N(\nu_s, \omega^2_s)$. This specification allows for the documented leptokurtic distribution of the effective spread (Hamilton, 1996; Das, 2002).[9]

The process for X_t has the following VAR representation:

$$X_{t+1} = \mu(I_{t+1}) + \Phi(I_{t+1}) X_t + \xi_{t+1}, \tag{11}$$

where the indicator I_{t+1} is equal to 1 if a FOMC meeting is scheduled at date $t+1$ and zero otherwise.[10] The process for X_t belongs to the family of affine processes (see Appendix A.2-A.3) but does not belong to the compound autoregressive family of Darolles, Gourieroux,

[9]Note that s_{t+1} does not respond to z_t and l_t. This is consistent with the Fed's explicit actions to counteract any predictable deviations of the effective rate from its target in this sample.

[10]Equation 11 can be estimated via Maximum Likelihood when X_t is observed.

and Jasiak (2006) because of the deterministic dependence on the meeting schedule. The conditional distribution of ξ_{t+1} is known. Its variance is constant except for its first element.

E Stochastic Discount Factor

The model is set in discrete time and markets are incomplete. In the absence of arbitrage opportunities, the risk-neutral measure exists but it is not unique. Consider the family of exponential-affine SDF M_{t+1}:

$$M_{t+1} = \exp\left(-r_t^{eff}\right) \frac{\exp(\delta_t^\top X_{t+1})}{E_t\left[\exp\left(\delta_t^\top X_{t+1}\right)\right]}, \tag{12}$$

where δ_t is the vector of prices of risk. The compensation for risk is determined by the prices of risk δ_t,

$$\delta_t = \delta_0 + \delta_1 X_t. \tag{13}$$

This family nests a wide range of equilibrium-based SDFs (Gourieroux and Monfort, 2007). The effective rate r_t^{eff} is the relevant overnight rate for money market participants: the target rate is only a target and most transactions occur at the effective rate.

F Risk-Neutral Dynamics

The price of target risk is constant. Target rate risk will still generate significant risk premium variations since variance and skewness are time-varying (see Section D). The dynamics for X_t are affine under the risk-neutral measure (Appendix A.4). In fact, the dynamics for X_t have the same form under the historical and risk-neutral measures. The target rate has the same conditional distribution, with intensity parameters given by

$$\lambda_{0,u}^Q = \lambda_{0,u} \exp(\delta_{0,r}\Delta) \qquad \lambda_{0,d}^Q = \lambda_0 \exp(-\delta_{0,r}\Delta), \tag{14}$$

when there is no FOMC meeting and

$$\lambda_u^Q = \lambda_u \exp(\delta_{0,r}\Delta) \qquad\qquad \lambda_d^Q = \lambda_d \exp(-\delta_{0,r}\Delta), \tag{15}$$

when there is a FOMC meeting.

G Asset Pricing

Consider a federal funds futures contract that settles at the end of a reference calendar month n. This contract pays off the difference between the contract rate and the average overnight federal funds rate in the reference month $\bar{r}_n$. With no loss of generality, the notional of the contract is 1. Futures contracts require no investment at inception. The futures rate $F(t,n)$ is equal to the discounted value of its payoff:

$$\begin{aligned} F(t,n) &= E_t\left[M_{t,t+T_n}\bar{r}_n\right] = E_t\left[M_{t,t+T_n}D_n^{-1}\sum_{i=T_n-D_n}^{T_n} r_{t+i}\right] \\ &= D_n^{-1}\sum_{i=T_n-D_n}^{T_n} E_t\left[M_{t,t+T}r_{t+i}\right] \\ &= D_n^{-1}\sum_{i=T_n-D_n}^{T_n} f(t,i,T_n), \end{aligned} \tag{16}$$

where T_n is the number of days between t and the end of month n and D_n is the number of days in month n.[11] Proposition 1 shows that the rate of a singleton futures contract $f(t,i,T_n^*)$ is not linear. This will be accounted for at estimation.

LIBOR loans are short-term, unsecured interbank loans and investors require an extra

[11] The quoted price of this contract, $P(t,n)$, is given by $P(t,n) = 100 - F(t,n)\times 3600$. Because of weekends or holidays, the settlement date $t+T_n^*$ may not coincide with the last day of the month $t+T_n$. Proposition 1 uses $T^* = T$ for simplicity but estimation accounts for this difference.

Proposition 1 *Price of a Singleton Futures Contract*

Take $0 \leq t \leq h \leq T$. The rate at time-t of a singleton futures contract $f(t,h,T)$ for the reference day $t+h$ and that settles at date $t+T$ is

$$\begin{aligned} f(t,h,T) \equiv & E_t\left[M_{t,t+T} r_{t+h}\right] = \frac{\partial}{\partial u} E_t\left[M_{t,t+T}\exp(u r_{t+h})\right]\Big|_{u=0} \qquad (17) \\ = & \exp\left(d_0^{rf}(t+h,T-h) + c_0\left(u^*,t,h\right)\right) + c\left(u^*,t,h\right)^\top X_t\Big) \\ & \times \left[c_0^{'}\left(u^*,t,h\right) C_r + X_t^\top c^{'}\left(u^*,t,h\right) C_r\right]. \qquad (18) \end{aligned}$$

See Appendix B.4 for the proof and details of the coefficients.

yield to hold them. From Equation 8, the price of a LIBOR loan is given by

$$D^l(t,m) \equiv E_t\left[M_{t,t+m}\exp\left(-\sum_{i=0}^{m-1} l_{t+i}\right)\right] = \exp\left(d_0^L(t,m) + d^L(t,m)^\top X_t\right), \qquad (19)$$

with coefficients given in Appendix B.3. Figure 1 compares futures and forward LIBOR rates. It shows that LIBOR rates on loans initiated in 1999 jumped upward when their maturity first extended into 2000. Drossos and Hilton (2000) document the impact of Y2K fears on LIBOR rates (see also Sundaresan and Wang, 2009). Banks placed a greater value on being liquid or charged more for counterparty risk on the last day of the 20th century. A dummy variable is introduced to capture this effect. The Millennium premium l^* is defined through the following modification of the LIBOR loan equation:

$$D^L(t,m) = E_t\left[M_{t,t+m}\exp\left(-\sum_{i=0}^{m-1} l_{t+i} + l^* I(t+i,m)\right)\right],$$

where the indicator $I(t,m)$ is equal to 1 if $t < t^* \leq t+m$ and 0 otherwise and t^* is the last business day of 1999.

II Data and Estimation

A Data and Summary Statistics

The sample includes daily data on the target and effective overnight funds rate at the Fed; daily data on federal funds futures contracts with horizons from 1 to 6 months; and daily data on LIBOR loans with maturities of 1 to 12 months. Daily changes in futures rates around FOMC decisions identify policy shocks during estimation. LIBOR rates provide a natural term structure associated with the overnight market since they correspond to the rates at which large banks are prepared to lend to each other on an unsecured basis. I exclude futures contracts with horizons beyond 6 months since they are relatively illiquid for most of the sample. More details on the data are provided in Appendix C.1.

The sample starts at the beginning of 1994 when the Fed first used discrete 0.25 percent increments explicitly. The sample ends in July 2007. The analysis consciously ignores several important but confounding issues present in the data starting in 2008. The Fed introduced a structural change to the effective overnight rate market since 2008. Allowing the effective rate to move in a range between 0 and 0.25 percent implies a structural break in the equation for the effective spread s_t. More importantly, the target rate reached a zero lower bound in the United States. Finally, the Fed introduced long-term asset purchases and changed its communication of forward guidance in a few instances. Restricting the sample to the pre-crisis period highlights the relationship between anticipations and uncertainty about future policy decisions in a "normal" sample.

Table 1 presents summary statistics. The average term structures of LIBOR and forward rates are upward sloping but the forward curve is steeper. The term structure of LIBOR volatilities is almost flat, with a slight humped shape at intermediate maturities. The term structure of futures is lower and flatter than that of the LIBOR rates. Table 1(d) provides summary statistics for the spreads between LIBOR forward rates and futures rates.

The forward-to-futures spreads vary substantially and contain significant information about future excess returns.

B The Information Content of Forward-to-Futures Spreads

Combining futures and LIBOR forward rates generates information about future excess returns. This information can be summarized with two components. Table 2 reports results from a principal components analysis of forward-to-futures spreads across maturities.[12] The first two components explain 66 percent of the total variance. The pattern of loadings on each of these components indicates that they signal changes in the level and slope of the spreads across maturities, respectively. Higher-order components reflect idiosyncratic variations around specific points along the term structure.

I use predictability regressions to measure the information content of forward-to-futures spreads for excess returns from holding a futures contract.[13] Excess returns from holding the futures contract for calendar month n during one month are given by

$$xr_{t,n} = F(t,n) - F(t+m,n). \tag{20}$$

The predictive regressions combine the level and slope components of forward-to-futures spreads:

$$xr_{t,n} = \gamma_{0,n} + \gamma_{lvl}\ level_t + \gamma_{slp}\ slope_t + u_{t,n}. \tag{21}$$

Table 3 presents the results.[14] The level is never significant, but the slope is significant for

[12]The analysis excludes the last nine months of 1999 owing to fear of the Millennium change in the interbank market (See Section G above).

[13]Piazzesi and Swanson (2008) show that accounting for variation margins due to marking positions to market prices produces near-identical excess returns (see the working paper version of their article).

[14]The monthly returns do not overlap. Standard asymptotic inference remains valid (Richardson and Stock, 1989; Valkanos, 2002; Diez de los Rios and Sentana, 2011). Moreover, the regressors' persistence cannot be driving the results along the lines in Stambaugh (1999). Assuming that the level and slope factors follow AR(1) processes, estimates of the persistence coefficients are 0.66 and 0.50, respectively, and estimates of the correlations between AR(1) innovations and residuals from predictive regressions range between -0.10 and -0.35 for the level factor and -0.06 and 0.20 for the slope factor. On the other hand, the results are conservative, since short-horizon returns are noisy relative to the ex-ante risk premium.

contract maturities of three months or more. Increasing the slope by one standard deviation increases expected monthly excess returns by 5 to 7 basis points (bps), annualized. This is economically significant relative to average excess returns of 2 and 4 bps. Table 3(b) shows similar results for excess returns on forward rates. Hence, forward-to-futures spreads predict excess returns and can be used to improve policy rate forecasts. This justifies combining forwards and futures in a dynamic term structure model.

There are several reasons why futures and LIBOR markets may not be fully integrated and reveal different information. LIBOR loans are fully funded while futures contracts require no exchange of principal. In addition, LIBOR loans are uncollateralized, while futures contracts are cleared via a central counterparty where variation in margins minimizes the default exposures of each participant. Finally, participation in the LIBOR market is limited to large banks and LIBOR positions cannot be reversed as easily when funding conditions worsen.

C Estimation

The model is estimated using its state-space representation. A brief description is given here and details of the estimation procedure are provided in Appendix C. The VAR representation in Equation 11 provides the transition equation for the state vector X_t, which includes the two latent states z_t and l_t. The latent states are filtered based on observed LIBOR rates and futures rates, stacked in vector Y_t. The vector Y_t is combined with observed target and effective overnight rates in the measurement vector $\tilde{Y}_t = [r_t \; s_t \; Y_t^\top]^\top$. The history of observable variables for $t = 1, \ldots, t$ is summarized by $\tilde{Y}_{\underline{t}}$ (with $\tilde{Y}_{\underline{0}}$ an empty set).

All futures and LIBOR rates are measured with i.i.d. Gaussian errors. The Unscented Kalman Filter (UKF) is used to recover estimates of the latent variables. The UKF is an approximate filter that matches the first two moments of the state distribution. This filter accounts for nonlinearities in the measurement equations due to futures rates. Conditional on filtered estimates of the latent variables, the joint conditional likelihood of the data is

given by

$$
\begin{aligned}
L(\Theta; Y_{\underline{T}}) &= \sum_{t=1}^{T} \log \left(f \left(\tilde{Y}_t | \tilde{Y}_{\underline{t-1}}, I_t; \Theta \right) \right) \\
&= \sum_{t=1}^{T} \log \left(f(Y_t | \tilde{Y}_{\underline{t-1}}, I_t) f(r_t | \tilde{Y}_{\underline{t-1}}, s_t, I_t) f(s_t | s_{t-1}) \right),
\end{aligned}
$$

where all model parameters are grouped in the vector Θ. The likelihoods of Y_t and r_t depend on the deterministic FOMC schedule via the indicator I_t.

D Specification

Standard identification and stationarity assumptions are discussed in Appendix C.4. The following additional restrictions are implemented at estimation for parsimony and simplicity. The parameters λ_0^u and λ_0^d are poorly estimated because of the lack of policy changes outside of scheduled FOMC meetings. These are calibrated such that the distribution of target changes is symmetrical outside of scheduled FOMC meetings and that the variance of target changes matches the sample variance. Results are robust to the choice of calibration strategy. This approach is similar to the calibration in Piazzesi (2005a). In addition, the FOMC does not respond to the current spread when deciding its target for the overnight rate ($\lambda_{u,s} = \lambda_{d,s} = 0$). Then, the marginal likelihood of s_t can be separated so that its parameters can be estimated separately in a first stage.[15]

The following restrictions on the parameters of the prices of risk make interpretation of the results easier. First, the price of risk for z_t is left unrestricted. The empirical results attribute all variations in the price of risk to the cyclical path factor, which captures information about future target rate changes. The price of target rate risk is constant. This helps disentangle the effect of varying quantities of risk on the risk premium from the effect of varying the

[15]Results are essentially unchanged if we proceed via joint estimation. On the other hand, a separate estimation lightens the computation burden, improves numerical optimization and leads to a more accurate Hessian matrix because of the weak link between s_t and yields in the data.

price of target rate risk (see Equation 22 in the Results). The price of risk for l_t is constant. This restriction enforces the identification of that factor with the forward-to-futures spreads, which is usually directly interpreted as a risk premium. The price of risk for s_t is also constant. In other words, the vector δ_0 is left unrestricted but the matrix δ_1 has zeros everywhere except on the third row (which corresponds to the position of z_t).

III Results

A Pricing Errors

Table 4 presents mean pricing errors (MPE) and root mean squared pricing errors (RMSE) in Panel (a) and Panel (b), respectively. The model provides a good fit with little bias if any. Average errors are typically less than 1 bps and often less than one-tenth of 1 bps across maturities. LIBOR RMSE is 4.3 bps across all maturities. Piazzesi (2005a) reports average absolute errors of 12.5, 7.5 and 6.8 bps for LIBOR rates at maturities of 1, 3 and 12 months, respectively. This compares with 6, 4 and less than 1 bps here. Futures RMSE is 8.8 bps overall and increases with maturity, from 3 to 12 bps.[16]

B The Path Factor

Figure 2(a) reports filtered estimates of the path factor along with the target rate. The path factor filtered from the cross-section of federal funds futures captures forward-looking information about future FOMC decisions. To give a sense of how target rate forecasts change from the model change with the path factor, consider varying the path factor but keeping other variables constant. At the median value of the path factor, the change forecast is essentially 0. At the average value in the lower tercile, the change forecast is around -10 bps, but at the average value in the higher tercile, the change forecast is around +15 bps.

The Fed's dual mandate suggests that the path factor aggregates information about real activity and inflation. To see the relationship with real activity, Figure 2(b) compares the

[16]Estimates of pricing error variance parameters (unreported) are consistent with sample RMSEs.

path factor with the Aruoba-Diebold-Scotti (ADS) index of US real activity.[17] The positive relationship is visually apparent. The path factor is strongly cyclical. In addition, the path factor leads the ADS index for several months ahead but the ADS index and the path factors diverge in a few instances. As one example, the ADS index declined sharply in 2000 but the path factor did not.

These divergences occur because the path factor z_t aggregates additional relevant information. For a start, the FOMC must also consider information related to inflation. Indeed, the divergence in 2000 provides a case in point where z_t contains key conditioning related to inflation. To show this, we can use the FOMC statements and transcripts to analyze the narratives of the events.

The path factor rose and diverged from the ADS index to signal that the FOMC would raise its target rate. Indeed, the target rose to a high of 6.5 percent at the FOMC meeting on 16 May 2000. The FOMC statement for that meeting emphasized inflation risk over unemployment. As late as 15 November, the FOMC noted that "the risks continue to be weighted mainly toward conditions that may generate heightened inflation pressures in the foreseeable future." They emphasized inflation pressures even if they also noted that "softening in business and household demand and tightening conditions in financial markets over recent months suggest that the economy could expand for a time at a pace below [...] its potential to produce."

Later on, between November and December, the path factor fell rapidly, anticipating a change of tone. Indeed, the statement on 19 December 2000 shifted the risk assessment. The FOMC left inflation aside but stated that "the risks are weighted mainly toward conditions that may generate economic weakness in the foreseeable future."[18] On 3 January 2001, the

[17]The Philadelphia Fed publishes the index daily and describes it as "designed to track real business conditions at high frequency. Its underlying economic indicators (weekly initial jobless claims; monthly payroll employment, industrial production, personal income less transfer payments, manufacturing and trade sales; and quarterly real GDP) blend high- and low-frequency information and stock and flow data."

[18]The FOMC also noted that "rising energy costs, as well as eroding consumer confidence, reports of

FOMC finally lowered its target for the federal funds rate by 50 bps, following an unscheduled conference call.[19] The path factor filtered from futures anticipated this change of direction.

For completeness, Figure 2(c) compares the path factor z_t and the forward-to-futures spreads factor l_t. The spread and path factors are strongly negatively correlated. By construction, filtered estimates of l_t are closely connected to the spreads between futures and LIBOR forward rates. The LIBOR spread and other credit spreads are generally are countercyclical. Unsurprisingly, we find that l_t rises when z_t falls; that is, when economic conditions deteriorate. Section G discusses the information content of the forward-to-futures spread l_t in greater detail.

C Time-Varying Volatility of Unexpected Target Changes

From Equation 4, the state variables X_t drive the volatility of unexpected FOMC target changes. The sign and strength of this relationship are determined by the $\lambda_u - \lambda_d$ parameters. Looking at the estimates in Table 5, one can see that $\lambda_{z,u} \ll \lambda_{z,d}$ but that $\lambda_{r,u} \approx \lambda_{r,d}$, and $\lambda_{l,u} \approx \lambda_{l,d}$. In the results, the path factor z_t drives the volatility of unexpected FOMC target changes.

To see this, the sample was first split into three terciles of the path factor and then each subsample was split using terciles of the target rate within each macro tercile. This produces nine subsamples accounting for the observed comovements of the path factor and the target rate. For example, the three subsamples (*Low, Low*), (*Low, Median*) and (*Low, High*) vary the target rate from low to high values, conditional on the path factor being low.

Panel (a) of Figure 3 reports the average conditional volatility in each subsample. Each line corresponds to a tercile of the path factor. The results show large variations. The

substantial shortfalls in sales and earnings, and stress in some segments of the financial markets suggest that economic growth may be slowing further." Interestingly, the path factor reached a low point on the day of the meeting and rose in the following weeks.

[19]The tightening episode in 2003–2004 offers another case. The path factor again lagged behind the ADS index for some time when FOMC cited low inflation and delayed its response to improving economic conditions.

volatility of unexpected FOMC target changes is highest when the path factor signals a loosening cycle, ranging from 30 to 25 percent for different levels of the target rate. Volatility declines to around 20 percent for median values of the path factor and to 10 percent for the highest values of the path factor, respectively. Raising the target rate also lowers the volatility, but the effect is much smaller.

Panel (b) shows the average conditional skewness of unexpected FOMC target change in each sub-sample. Skewness is high and positive, between 4 and 5.25, when the path factor is high. Otherwise, skewness is close to 0 when the path factor is low or close to its median value .[20] Therefore, a high value of the path factor signals a distribution of potential changes that is narrow and clearly skewed toward an increase. In contract, a low value of the path factor signals a wide distribution with a slight skew toward a decrease.

Do the risk premiums respond to as the volatility moves from low to high? To answer this question, I first divide the sample based on terciles of the target rate and then based on tercile of conditional volatility. Panel (c) shows the risk premium on a 6-month futures contract in different subsamples, where the average risk premium is substracted. Panel (c) shows that raising the target rate lowers the risk premium for every level of volatility. Fixing the conditional volatility to its median value, the risk premium decreases by around 10 bps between low and high levels of the target rate (on average). By contrast, varying the volatility only affects the risk premium for when the target rate is high. Fixing the level of the target at its top tercile value, the risk premium *increases* by more than 10 bps between low and high volatility (on average). Hence the transmission from volatility to the risk premium arises mostly in the early stages of a recession.

Changes in the expected path of the target rates affect variance and skewness in the opposite direction (i.e., high variance but low skewness). To see the net effect, Figure 4 shows the conditional distribution of unexpected FOMC target changes. Three panels report the

[20]Note that the model inherits from the Poisson distribution that excess kurtosis is inversely related to variance (and strictly positive).

distribution given different economic conditions. Panel 4(a) reports the distribution in the (*Low, Low*) subsample, conditioning the distribution on the average value of the target and path variables in this sample. Similarly, Panel 4(b) and Panel 4(c) report the distribution in the (*Median, Median*) and the (*High, High*) subsamples. These panels tell a simple story. A downward path for future target rates is associated with greater uncertainty surrounding upcoming FOMC decisions. An upward path is associated with lower variance primarily by shutting down the probability of a target cut. The asymmetrical effect generates positive skewness. It is a smaller left side of the distribution that is driving skewness higher (not a larger right side of the distribution).

D Compensation for Risk

The signal from the path factor affects the risk premium via two mechanisms. The first mechanism is common. Innovations to the path factor signal rising interest rates and the effect on the risk premium depends on variations in the prices of risk, which represents changes in marginal utilities. The second mechanism is different. The path factor signals lower uncertainty around future changes to the target rate. This also affects the risk premium even if the price of target rate risk is constant.

To understand the compensation for risk associated with the SDF in Equation 12, consider a portfolio with payoff $\exp(-c^\top X_{t+1})$ where c is the vector of risk exposures. The expected excess return (continuously compounded) on this portfolio is

$$E_t^{\mathbb{P}}\left[\log \frac{\exp(-c^\top X_{t+1})}{E_t[\exp(-r_t - c^\top X_{t+1})]}\right] = -c^\top Var_t^{\mathbb{P}}[X_{t+1}]\delta_t + o(c) + o(\delta_t). \tag{22}$$

(See Le, Singleton, and Dai, 2010, p.2199.) The compensation for risk is affected by changes in the prices of risk δ_t or changes in the quantity of risk $-c^\top Var_t^{\mathbb{P}}[X_{t+1}]$, where only the first row in the variance term varies over time. Consider the compensation for exposures to target rate risk: $c^\top = [1\ 0\ 0\ 0]$. The compensation for target risk is driven by $-Var_t^{\mathbb{P}}[r_{t+1}] \times \delta_{0,r}$

and $-Cov_t^{\mathbb{P}}[r_{t+1}, z_{t+1}] \times \delta_{z,t}$.[21]

Consider the first term $-Var_t^{\mathbb{P}}[r_{t+1}] \times \delta_{0,r}$. The price of target rate risk $\delta_{0,r}$ is negative and significant. Changes to the FOMC target that are higher than expected are associated with higher marginal utility states. This may reflect the oft-cited fears that the Fed will either increase the target rate too much (when tightening) or not decrease it enough (when loosening). In the model, this channel shifts the dynamics of r_t under the risk-neutral measure $\mathbb{Q}$ relative to the $\mathbb{P}$ measure. This shift is given by Equation 15, in which the multiplying factors are $\exp(\delta_{0,r}\Delta) \approx 0.95$ and $\exp(-\delta_{0,r}\Delta) \approx 1.05$.[22] Therefore, the compensation for target rate risk pulls the components of λ_u closer to 0 and pushes the components of λ_d away from 0. Since $\lambda_d > \lambda_u$ and the adjustments $\exp(\delta_{0,r}\Delta)$ and $\exp(-\delta_{0,r}\Delta)$ are multiplicative, this channel works mainly through an increase in the response of the target rate to the path factor under the risk-neutral measure. Then, shifting the path signal also drives the futures contract rates away from the Expectation Hypothesis, generating risk premium variations.

Consider the second channel affecting compensation for target rate risk, $-Cov_t^{\mathbb{P}}[r_{t+1}, z_{t+1}] \times \delta_{z,t}$. This channel is standard, working via the price of path risk $\delta_{z,t}$ and the covariance between level and path. This covariance is positive. Table 5(d) reports parameters for the price of risk $\delta_{z,t}$. The price of path risk is positive, on average, implying that an unexpected upward shift to the path of future target rates is associated with high marginal utility states, on average. All the components of $\delta_{1,z}$ are statistically significant. Economically, z_t and l_t are the significant drivers. The price of risk increases when the path itself declines, which is consistent with the interpretation of a path decline signaling worsening economic conditions. In addition, the price of path risk increases with an increase in the spread between the LIBOR forward rate and futures spreads. The price of path risk also increases when the

[21] This is an approximation because higher-order moments of target changes also vary. Fontaine (2014) shows that a constant price of target risk can generate significant risk premium variations in a case with constant variance because of the changing skewness in target rate changes. Polimenis (2006) discusses the effect of skewness on the risk premium in economies with power utilities.

[22] That is, $\exp(\pm 7.47 \times 10^3 \times 0.25/36000)$.

target rate is lower, but this effect is small.

E Forecasting Target Rates

This section assesses the accuracy of the target rate forecasts as a check of the ability of the model to disentangle the risk premium. The excess returns obtained from holding a futures contract referencing month n from time-t until its maturity are given by

$$xr_{t,n} = F(t,n) - \bar{r}_n = F(t,n) - E_t[\bar{r}_n] - \epsilon_{t,n}, \tag{23}$$

where $xr_{t,n}$ are the excess returns. Equation 23 shows that the combination of the low futures pricing errors and accurate target rate forecasts implies an accurate description of the risk premium in futures rates. The next section discusses this risk premium.

A time-t forecast of the effective overnight rate at date $t+h$ with $h > 0$ is given by

$$E[r_{t+h} + s_{t+h}|X_t] = a_{r+s}(I_{t+1}, h) + b_{r+s}(I_{t+1}, h)^\top X_t, \tag{24}$$

with coefficients $a_{r+s}(\cdot)$ and $b_{r+s}(\cdot)$ given in Appendix D.2. For comparability with existing results, I focus on forecasts of the average rate in calendar month n. The predicted average overnight rate for calendar month $\bar{r}_n$ is given by $E[\bar{r}_n|X_t] = D_n^{-1} \sum_{i=1}^{D_n} (r_{t+h} + s_{t+h})$, where D_n is the number of days in month n.

As benchmark models, I use predictive regressions based on futures and LIBOR forward rates. Krueger and Kuttner (1996) use futures rates to forecast target rates. Gurkaynak, Sack, and Swanson (2012) show that futures deliver the best (lowest RMSE) market-based forecasts of $\bar{r}_n$ up to six months ahead. Similarly, LIBOR rates deliver the best forecasts at longer horizons, up to a year. Chun (2011) shows that futures deliver the best forecasts relative to surveys of professional forecasters and time-series models. Benchmark forecast

models are given by

$$\begin{aligned} E[\bar{r}_n|X_t] =& \bar{a}(t,n) + \bar{b}(t,n)^\top X_t \\ E^{fut}[\bar{r}_n|X_t] =& \alpha_h^{fut} + \beta_h^{fut} F(t,n) \\ E^{lib}[\bar{r}_n|X_t] =& \alpha_h^{lib} + \beta_h^{lib} F_{lib}(t,n), \end{aligned} \tag{25}$$

where $F(t,n)$ and $F_{lib}(t,n)$ are the futures and forward LIBOR rates for calendar month n. Coefficients $\bar{a}(t,n)$ and $\bar{b}(t,n)$ are obtained from the estimation results above. Coefficients of the predictive regressions can be estimated via ordinary least squares (OLS). The time-series of monthly averages $\bar{r}_n$ is regressed on a forward or futures rate observed h days before the beginning of each month.[23] I consider horizons $h = 1, 2, \ldots, 178$ days when using futures rates and $h = 1, 2, \ldots, 360$ days when using forward rates. There are no overlapping observations. The regression estimates minimize forecasting errors for each horizon separately and may suffer from in-sample over-fitting. On the other hand, predictive coefficients from the term structure model are computed from parameter estimates obtained from fitting the cross-section of futures and forward rates. This mitigates the impact of over-fitting on no-arbitrage forecasts.

Figure 5(a) compares forecast RMSEs. Figure 5(b) compares the corresponding R^2s. Both figures also report results from random walk forecasts. Every predictor improves RMSEs substantially relative to random walk forecasts. Futures outperform other forecasts at short horizons. At a horizon of 50 days, RMSEs are 10 bps for futures-based forecasts and 15 bps in the case of forward or model-based forecasts. In all cases, R^2s are very close to 1. However, the advantage of futures deteriorates at longer horizons. At a horizon of six months, RMSEs are slightly above 45 bps for each predictor. At longer horizons, model-

[23] Model-based and futures-based forecasts exactly match the calendar month for any horizon h. On the other hand, the reference periods underlying forward rates have small variations in overlap for different h. This induces small RMSE variations across horizons. However, the overlap is constant for a given horizon (regression) and the match is exact for a subset of horizons.

based forecasts provide improvements over forward-based forecasts. One year ahead, R^2s are 63 and 60 percent, respectively.[24]

Figure 6 reports the time series of forecasting errors averaged across a range of horizons. Averaging across horizons removes some of the noise in regression-based forecasts due to daily idiosyncratic variations in individual futures and forward rates. Panel (a) compares errors over horizons between 3 and 6 months. Consistent with the results in Figure 5, futures offer small benefits at these horizons. Panel (b) covers horizons between 6 and 9 months and Panel (c) covers horizons between 9 months and 1 year. Model-based forecasts are generally lower and less cyclical. The mean absolute errors of model forecasts are 17 bps lower than forward-based forecasts at horizons between 6 and 9 months and 22 bps lower at horizons between 9 and 12 months. This significant improvement is of the same magnitude as the typical target rate change.

Forecast errors can be large and persistent for every model. Any forecasting model is bound to produce cyclical errors at horizons several months ahead, since some of the target rate changes were truly unpredictable six months or one year in advance. Nonetheless, forecasts from the model are unbiased. Average forecasting errors range between -2.4 and 2.7 bps across horizons and the associated t-statistics for the null of unbiased forecasts, accounting for autocorrelation up to 12 lags, are always far from the usual significance levels. The only exceptions are for horizons of a few days, in which economically tiny average errors, around 0.2 bps, appear statistically significant.

F Risk Premium

The results provide an accurate description of the forecast and risk premium components in Equation 23. It provides accurate and unbiased target rate forecasts, capturing properties of the historical dynamics. It delivers low pricing errors, capturing properties of the risk-

[24]Results using futures and forward rates are comparable with those of Gurkaynak et al. (2012) in a shorter sample period and a longer quarterly sampling frequency.

neutral dynamics. Therefore, the model provides a credible measure of the risk premium implied in futures rates.[25] Figure 7 compares the conditional risk premium with ex-post realized returns from holding the 6-month-ahead contract (i.e., $E_t[xr_{t,6}]$ and $xr_{t,6}$).

Figure 7 also shows a few instances of large and persistent gaps. These gaps between realized excess returns and the risk premium are the unexpected component in $\bar{r}_n$ ($\epsilon_{t,n}$ in Equation 23). These cases with large returns in excess of the risk premium do not provide evidence against the model risk premium. For example, large excess returns toward the end of 1994 can be attributed to the Mexican peso crisis, which contributed to an unexpected pause in Fed's tightening cycle and to the subsequent target rate cuts. Moreover, large returns in 1998 can be attributed to the unforeseen collapse of Long-Term Capital Management and the subsequent response by the Fed. A few gaps appear to be associated with unforeseen developments in the real economy, for example, target cuts during the 2001 recession and following the terrorist attacks of September 2001.[26]

In terms of magnitude, the risk premium on the 6-month contracts (which is shown in Figure 7) can vary substantially. The risk premium can spend long periods close to zero, but the risk premium often stays around 25 bps for extended periods and even reaches 50 bps on a few occasions. In other words, the risk premium can vary by one or two rate changes over the course of the monetary cycle. This is economically significant.

G The Information Content in the Spread Factor

The spread factor l_t captures the information contained in the spreads between LIBOR forward rates and federal funds futures rates. The parameter estimates imply that the spread factor influences the price of path risk $\delta_{z,t}$. Therefore, the spread factor also influences the risk premium in futures rates. The information content in the spread factor originates in the

[25] Ferrero and Nobili (2008) use surveys of professional forecasters to compute the ex-ante premium and ex-post forecast errors. However, these forecasts appear biased. See their Table 4).

[26] Hamilton and Okimoto (2011) identify two regimes in futures excess returns. The episodes discussed here correspond to periods with high probabilities of a regime with higher mean and volatility of returns.

exchange-traded futures market or in the interbank LIBOR market. The spread can widen because of worsening credit or funding conditions on the interbank market. The spread can also widen if transaction costs or limits to arbitrage in the futures market allow predictable price pressures. Both channels are consistent with a negative correlation of the spread factor with future target rates. Higher LIBOR rates today may predict lower target rates because of the future FOMC's response to funding risk. Lower futures rates today may predict lower target rates because hedging demand pressures on futures rates reveal lower investors' forecasts.

However, these two channels can be differentiated empirically based on their opposite implications for excess returns. Hedging demand pressure also predicts *lower* excess returns on the futures markets. Funding risk in LIBOR rates that predicts lower target rates also predicts *higher* excess returns on the LIBOR market. I test the first hypothesis via predictive regressions for futures excess returns:

$$xr_{t,n}^{Fut} = \gamma_{0,n} + \gamma_{l,n} l_t + u_{t,n}, \tag{26}$$

where l_t is the spread factor and we should have $\gamma_{l,n} < 0$. I test the second hypothesis via similar predictive regressions but for forward rates returns:

$$xr_{t,n}^{For} = \gamma_{0,n} + \gamma_{l,n} l_t + u_{t,n}, \tag{27}$$

where we should have $\gamma_{l,n} > 0$. As in Section B, excess holding returns are computed at a monthly frequency without overlapping observations. Table 6 displays the results.

Panel (a) reports results for futures excess returns. Monthly excess returns averaged between 2 and 4 bps (annualized) across maturities. These are consistent with results in Hamilton (2009). The information content of liquidity is significant and large. Coefficients have the expected sign. A one standard deviation increase in the spread factor decreases

excess returns between 3 and 6 bps for maturities beyond two months. The R^2 ranges from 5 to 7 percent. Panel (b) reports results for forward excess returns. Results show no evidence of predictability from the spread factor. Coefficients typically have the wrong sign. The evidence points toward transitory hedging demand pressures on the futures market as the main channel to explain the information content of the spread.

H The Role of Hedging Demand

Piazzesi and Swanson (2008) show that futures excess returns can be predicted using net long positions of non-commercial participants on the futures market. They argue that "hedgers–primarily banks–essentially paid an insurance premium to non-commercial participants for providing hedging services." An important question is whether the information content of the spread factor is shared with variations in the net long positions of non-commercial hedgers (NLP_t).[27]

Table 7 reports results from predictive regressions of futures excess returns on different combinations of the spread factor l_t, the path factor z_t and NLP_t. Panel (a) shows that the predictive content of NLP_t is similar to that of l_t, with R^2 ranging between 2 and 6 percent. Consistent with Piazzesi and Swanson (2008), NLP_t is positively correlated with excess returns. A one standard deviation increase predicts increases in returns of between 2 and 6 bps across maturities. Panel (b) presents results from regressions combining l_t and NLP_t. The R^2s are higher, ranging between 7 and 9 percent between maturities of three and six months but less than the sum of the univariate R^2s. Similarly, coefficient estimates are lower relative to univariate regressions. This suggests that these predictors overlap substantially. Finally, Panel (c) presents results from regressions combining l_t and z_t and NLP_t. Strikingly, combining macro conditions and hedging demand captures the information content of the spread factor. This is significant. Conditional on the path of future target changes, hedging

[27] I follow Piazzesi and Swanson (2008) and use eurodollar futures position data. The position data are published weekly with a three-day lag by the US CFTC. I match the daily data with the weekly CFTC mandatory reporting date to construct a weekly sample of factors, returns and positions.

demand captures the information content of the spread factor.

For comparison with existing results in Piazzesi and Swanson (2008), Table 7 reports results using hold-to-maturity excess returns. Our key message remains: hedging demand captures the information content of the spread factor. However, R^2s and the estimated coefficients are substantially higher, which is partly due to the overlapping structure in hold-to-maturity returns.

The evidence shows that hedging demand plays a predominant role in the information content of futures rates. Of course, the results do not preclude that funding risk in LIBOR rates affect the spread factor. Figure 2(c) clearly shows that the spread factor exhibits peaks at dates when financial markets were in turmoil. What the predictability results show is that variations of forward-to-futures spreads, which are informative for future target rates originated in the futures market in this sample.

IV Conclusion

This paper identifies the distribution of policy shocks using federal funds futures. This distribution is driven by a "path" factor signaling information about future target rates. These changes add substantial risk premium variations in money markets. The analysis consciously ignored several important but confounding issues, restricting the sample to the period between 1994 and 2007. First, extending the sample beyond 2007 requires a modification restricting the distribution of the target rate above a (possibly non-zero) lower bound. This could be achieved, for instance, via the function $\max(0, r_t)$ or by a quadratic specification of the change intensities λ_t^u and λ_t^d. Second, the Fed introduced a break in the behavior of the effective spread in 2009 when it announced that the overnight rate could move within a 0 to 0.25 percent range. Finally, the Fed combined forward guidance with long-term asset purchases in that period. We leave for future research whether and how these changes affect the level of uncertainty surrounding future FOMC decisions during recessions and expansions.

References

Ang, A., J. Boivin, S. Dong, and R. Loo-Kung (2011). Monetary policy shifts and the term structure. *The Review of Economic Studies 78*(2), 429–457.

Balduzzi, P., G. Bertola, and S. Foresi (1997). A model of target changes and the term structure of interest rates. *Journal of Monetary Economics 39*, 223–249.

Balduzzi, P., G. Bertola, S. Foresi, and L. Klapper (1997). Interest rate targeting and the dynamics of short-term rates. *Journal of Money, Credit and Banking 30*, 26–50.

Bansal, R., G. T. and H. Zhou (2004). Regime shifts, risk premiums in the term structure, and the business cycle. *Journal of Business and Economics Statistics 22*, 396–409.

Bernanke, B. and K. Kuttner (2005). What explain the stock market's reactions to Federal Reserve policy. *The Journal of Finance 60*, 1221–1257.

Christoffersen, P., C. Dorion, K. Jacobs, and L. Karoui (2014). Nonlinear Kalman filtering in affine term structure models. *Management Science 60*(9), 2248–2268.

Chun, A. L. (2011). Expectations, bond yields, and monetary policy. *Review of Financial Studies 24*(1), 208–247.

Cieslak, A. (2016). Short-rate expectations and unexpected returns in treasury bonds. Working paper, Duke University.

Cieslak, A. and P. Povala (2016). Information in the term structure of yield curve volatility. *The Journal of Finance 71*(3), 1393–1436.

Cochrane, J. and M. Piazzesi (2002). The Fed and interest rates : A high-frequency identification. *American Economic Review 92, P&P*, 90–95.

Cox, J., J. Ingersoll, and S. Ross (1985). A theory of the term structure of interest rates. *Econometrica 53*, 385–407.

Darolles, S., C. Gourieroux, and J. Jasiak (2006). Structural Laplace transform and compound autoregressive models. *Journal of Time Series Analysis 27*, 477–503.

Das, S. (2002). The surprise element: Jumps in interest rates. *Journal of Econometrics 106*, 27–65.

Diez de los Rios, A. and E. Sentana (2011). Testing uncovered interest rate parity: A continuous-time approach. *International Economic Review 52*(4), 1215–1251.

Drossos, A. S. and S. Hilton (2000). The Federal Reserves contingency financing plan for the century date change. *Current Issues in Economics and Finance 6*, 1–6. Federal Reserve Bank of New York.

Duffie, D., J. Pan, and K. Singleton (2000). Transform analysis and asset pricing for affine jump-diffusion. *Econometrica 68*, 1343–1376.

Duffie, D. and K. Singleton (1997). An econometric model of the term structure of interest-rate swap yields. *The Journal of Finance 52*, 1287–1321.

Eggertsson, G. B. and M. Woodford (2003). The zero bound on interest rates and optimal monetary policy. *Brookings Papers on Economic Activity*, 139–211.

Faust, J., E. Swanson, and J. Wright (2003). Identifying VARs based on high frequency futures data. *Journal of Monetary Economics 51*, 1107–1131.

Ferrero, G. and A. Nobili (2008). Futures contract as monetary policy forecasts. Technical Report 979, European Central Bank.

Fontaine, J.-S. (2014). Estimating the policy rule from money market rates when target rate changes are lumpy. In J. Chadha, A. Durré, M. Joyce, and L. Sarno (Eds.), *Developments in Macro-Finance Yield Curve Modelling*, Chapter 9, pp. 216–250. Cambridge: Cambridge University Press.

Gourieroux, C. and A. Monfort (2007). Econometric specification of stochastic discount factor models. *Journal of Econometrics 136*, 509–530.

Grammig, J. and K. Kehrle (2008). A new marked point process model for the federal funds rate target : Methodology and forecast evaluation. *Journal of Economic Dynamics & Control 32*, 2370–2396.

Grinblatt, M. (2003). An analytic solution for interest rate swaps. *International Review of Finance 2*, 113–149.

Gurkaynak, R., B. Sack, and E. Swanson (2005). Do actions speak louder than words? *International Journal of Central Banking 1*(1), 55–93.

Gurkaynak, R., B. Sack, and E. Swanson (2012). Market-based measures of monetary policy expectations. *Journal of Business and Economics Statistics 25*, 201–212.

Hamilton, J. (1996). The daily market for federal funds. *The Journal of Political Economy 104*, 26–56.

Hamilton, J. (2009). Daily changes in Fed funds futures prices. *Journal of Money, Credit and Banking 41*, 567–582.

Hamilton, J. and O. Jordà (2002). A model of the federal funds rate target. *The Journal of Political Economy 110*, 1136–1167.

Hamilton, J. and T. Okimoto (2011). Sources of variations in holding returns for Fed funds futures contracts. *Journal of Futures Markets 31*, 205–229.

Johannes, M. (2004). The statistical and economic role of jumps in coutinous-time interest rate models. *The Journal of Finance 59*, 227–260.

Johnson, N., S. Kotz, and N. Balakrishnan (1997). *Discrete Multivariate Distributions* (First ed.). New York Wiley.

Julier, S. and J. Uhlmann (1996). A general method for approximating nonlinear transformations of probability distributions. Robotics Research Group, University of Oxford.

Julier, S., J. Uhlmann, and H. Durrant-Whyte (1995). A new approach for filtering nonlinear systems. *The Proceedings of the American Control Conference 3*, 1628–1632. Seattle.

Krueger, J. and K. Kuttner (1996). The Fed funds futures rate as a predictor of Federal Reserve policy. *International Economic Review 16*, 865–879.

Krugman, P. (1998). Its baaack: Japans slump and the return of the liquidity trap. *Brookings Papers on Economic Activity*, 137–206.

Kuttner, K. (2001). Monetary policy surprises and interest rates: Evidence from the fed funds futures market. *Journal of Monetary Economics 47*, 523–544.

Le, A., K. J. Singleton, and Q. Dai (2010). Discrete-time affine$^{\mathbb{Q}}$ term structure models with generalized market prices of risk. *Review of Financial Studies 23*(5), 2184–2227.

Leippold, M. and L. Wu (2003). Design and estimation of multi-currency quadratic models. *European Finance Review 7*, 47–73.

Piazzesi, M. (2005a). Bond yields and the Federal Reserve. *The Journal of Political Economy 113*, 311–344.

Piazzesi, M. (2005b). *Handbook of Financial Econometrics*, Chapter "Affine term structure models". Elsevier.

Piazzesi, M. and E. T. Swanson (2008). Futures prices as risk-adjusted forecasts of monetary policy. *Journal of Monetary Economics 55*(4), 677 – 691.

Polimenis, V. (2006). Skewness corrections for asset pricing. Working paper, A. Gary Anderson Graduate School of Management.

Richardson, M. and J. Stock (1989). Drawing inference based on multiyear asset returns. *Journal of Financial Economics 25*, 323–348.

Rigobon, R. and B. Sack (2004). The impact of monetary policy on asset prices. *Journal of Monetary Economics 51*(8), 1553 – 1575.

Rogers, J., C. Scotti, and J. Wright (2016). Unconventional monetary policy and international risk premia. International Finance Discussion Paper 1172, Federal Reserve Board of Governors.

Rudebusch, G. (1998). Do measures of monetary policy in a VAR make sense? *International Economic Review 39*, 907–931.

Rudebusch, G. D. (2002). Term structure evidence on interest rate smoothing and monetary policy inertia. *Journal of Monetary Economics 49*(6), 1161–1187.

Sack, B. (2004). Extracting the expected path of monetary policy from futures rates. *International Economic Review 24*, 733–754.

Skellam, J. (1946). The frequency distribution of the difference between two Poisson variates belonging to different populations. *Journal of the Royal Statistical Society 109*, 296.

Stambaugh, R. F. (1999). Predictive regressions. *Journal of Financial Economics 54*(3), 375–421.

Stein, J. and A. Sunderam (2015). Gradualism in monetary policy: a time-consistency problem?

Sundaresan, S. and Z. Wang (2009). Y2K options and the liquidity premium in Treasury markets. *Review of Financial Studies 22*, 1021–1056.

Swanson, E. (2016). Measuring the effects of Federal reserve forward guidance and asset purchases on financial markets. Working paper, University of California, Irvine.

Swanson, E. T. (2006). Have increases in federal reserve transparency improved private sector interest rate forecasts? *Journal of Money, Credit and Banking 38*(3), 791–819.

Valkanos, V. (2002). Long-horizons regressions : Theoretical results and applications. *Journal of Financial Economics 68*, 201–232.

Wan, E. and R. V. der Merwe (2001). *Kalman filtering and neural network.*, Chapter "The unscented Kalman filter". Wiley and Sons.

Appendix

A Conditional Laplace Transform

A.1 Skellam Distribution

The dynamics of state variables are summarized by Equations 1, 9 and 10. Although the process for r_t is novel, its Laplace transform and its density are known in closed form. Conditional on the state, changes in the target rate follow a Skellam distribution (Skellam, 1946; Johnson et al., 1997). Consider two univariate Poisson variables N_1 and N_2 with parameters λ_1 and λ_2, respectively. The Laplace transform of their difference $Z \equiv N_1 - N_2$ is

$$T(u, Z) = \exp\left(\lambda_1(e^u - 1) + \lambda_2(e^{-u} - 1)\right), \quad u \in \mathbb{R},$$

while its probability mass function is

$$f(Z = z) = \exp(-(\lambda_1 + \lambda_2)) \left(\frac{\lambda_1}{\lambda_2}\right)^{z/2} I_z\left(2\sqrt{\lambda_1\lambda_2}\right),$$

where $I_z(\cdot)$ is the modified Bessel function of the first kind. In our context, the coefficients of the conditional Laplace transform vary through time because of the evolution of the underlying state variables and because of the deterministic variation in the FOMC meeting schedule. Hence, computation of the transform depends on the occurrence of an FOMC meeting in the next period, and the two cases must be treated separately.

A.2 No FOMC Meeting

The joint conditional transform when no meeting is scheduled to occur is given by

$$T(u, X_{t+1}|I_{t+1} = 0) \equiv E_t\left[\exp\left(u^\top X_{t+1}\right)|I_{t+1} = 0\right] = \exp\left(A(I_{t+1} = 0, u) + B(I_{t+1} = 0, u)^\top X_t\right),$$

where I_t is equal to 1 if a meeting occurs at time-t and 0 otherwise. Coefficients are given by

$$\begin{aligned} A(I_t = 0, u) &= g_0(u_r) + u^\top \mu(I_{t+1} = 0) + \frac{1}{2} u^\top \Omega u + \lambda_s\left(T(u_s, Y^s_{t+1}) - 1\right) \\ B(I_t = 0, z) &= \Phi(I_{t+1} = 0)u, \end{aligned}$$

where $\mu(I_{t+1} = 0)$ and $\Phi(I_{t+1} = 0)$ are defined in the text, and $g_0(x) \equiv \lambda_0^u(e^{\Delta x} - 1) + \lambda_0^d(e^{-\Delta x} - 1)$, and

$$\Omega = \begin{bmatrix} 0 & 0 & 0 & 0 \\ 0 & \sigma_s^2 & 0 & 0 \\ 0 & 0 & \sigma_z^2 & \sigma_{z,l} \\ 0 & 0 & \sigma_{z,l} & \sigma_l^2 \end{bmatrix}.$$

A.3 FOMC Meeting

The joint conditional Laplace transform in the case when an FOMC meeting is scheduled to occur, and conditional on the realization of s_{t+1}, z_{t+1} and l_{t+1}, is given by

$$\begin{aligned} T(u, X_{t+1}|I_{t+1} = 1) \equiv & E_t\left[\exp\left(u^\top X_{t+1}\right)|I_{t+1} = 1\right] = E_t\left[E_{s_{t+1}, z_{t+1}, l_{t+1}}\left[\exp\left(u^\top X_{t+1}\right)|I_{t+1} = 1\right]\right] \\ & = E_t\left[\exp\left(-G(u_r)^\top \bar{X} + \lambda(e^{\Delta u_r} + e^{-\Delta u_r} - 2) + G(u_r)^\top X^*_{t+1} + u^\top X^*_{t+1}\right)\right], \end{aligned}$$

where $X^*_{t+1} = [r_t\ s_{t+1}\ z_{t+1}\ l_{t+1}]$, the function $G(x)$ is given by

$$G(x) = [g_r(x)\ g_r(x)\ g_z(x)\ g_l(x)]^\top,\ x \in \mathbb{R},$$

and the functions $g_k(y)$ for $k = r, s, z$ are defined as

$$g_k(x) \equiv \left(\lambda_{u,k}(e^{x\Delta} - 1) - \lambda_{d,k}(e^{-x\Delta} - 1)\right).$$

We then have that

$$T(u, X_{t+1}|I_{t+1} = 1) = \exp\left(A(I_t = 1, u) + B(I_t = 1, u)^\top X_t\right),$$

with coefficients

$$\begin{aligned}
A(1,u) =& -G(u_r)^\top \bar{X} + h_1(u_r) + (G(u_r)+u)^\top \mu(I_{t+1}=1) + \frac{1}{2}(G(u_r)+u)^\top \Omega (G(u_r)+u) \\
&+ \lambda_s\left(T(g_s(u_r)+u_s, Y^s_{t+1}) - 1\right) \\
B(1,u) =& \Phi(I_{t+1}=0)(G(u_r)+u),
\end{aligned}$$

where $h_1(x) \equiv \lambda(e^{\Delta x} - 1) + \lambda(e^{-\Delta x} - 1)$.

A.4 Risk-Neutral Distribution

The joint conditional Laplace transform under $\mathbb{Q}$ is given by

$$\begin{aligned}
T^Q(u, X_{t+1}) &= E_t\left[M_{t,t+1}\exp\left(u^\top X_{t+1}\right)\right] \\
&= \exp\left(A^Q(I_{t+1}, u) + (B^Q(I_{t+1}, u) - C_r)^\top X_t\right),
\end{aligned}$$

where $C_r = [1\ 1\ 0\ 0]^\top$ and where coefficients are given by

$$\begin{aligned}
A^Q(0,u) =& g_0(u_r + \delta_{0,r}) - g_0(\delta_{0,r}) + u^\top(\mu(I_{t+1}=0) + \Omega\delta_0) + \frac{1}{2}u^\top\Omega u \\
&+ \lambda_s\left(T(u_s + \delta_{0,s}, Y^s_{t+1}) - T(\delta_{0,s}, Y^s_{t+1})\right) \\
A^Q(1,u) =& g_1(u_r + \delta_{0,r}) - g_1(\delta_{0,r}) - (G(u_r+\delta_{0,r}) - G(\delta_{0,r}))^\top \bar{X} \\
&- \frac{1}{2}G(\delta_{0,r})^\top \Omega G(\delta_{0,r}) + \frac{1}{2}(G(u_r+\delta_{0,r})+u)^\top \Omega (G(u_r+\delta_{0,r})+u) \\
&+ (G(u_r+\delta_{0,r})+u)^\top(\mu(I_{t+1}=1) + \Omega\delta_0) \\
&+ \lambda_s\left(T(g_s(u_r+\delta_{0,r}) + \delta_{0,s} + u_s, Y^s_{t+1}) - T(g_s(\delta_{0,r}) + \delta_{0,s}, Y^s_{t+1})\right)
\end{aligned}$$

and

$$\begin{aligned}
B^Q(0,u) &= (\Phi(I_{t+1}=0) + \Omega\delta_1)\, u \\
B^Q(1,u) &= (\Phi(I_{t+1}=1) + \Omega\delta_1)(G(u_r+\delta_{0,r}) - G(\delta_{0,r}) + u).
\end{aligned}$$

Moreover, the shift between risk-neutral and historical parameters is given by

$$\begin{aligned}
\mu^Q(0) &= \mu(0) + \Sigma\delta_0 & \mu^Q(1) &= \mu(1) + \Sigma(\delta_0 + G(\delta_{0,r})) \\
\Phi^Q(0) &= \Phi(0) + \Sigma\delta_1 & \Phi^Q(1) &= \Phi(1) + \Sigma\delta_1.
\end{aligned} \tag{28}$$

B Asset Prices

B.1 Generating Function for Prices

Proposition 2 provides the solution of the price-generating function $\Gamma(u,t,m)$ obtained from computing the time-t price of the generating payoff, $\exp(u^\top X_{t+m})$. Following Duffie et al. (2000), asset prices can be derived from $\Gamma(u,t,m)$. When $m=1$, $\Gamma(u,t,1)$ corresponds to the joint conditional Laplace transform of X_{t+1} under $\mathbb{Q}$.

Proposition 2 *Price-Generating Function*

In the absence of arbitrage opportunities, the time-t discounted value of the generating payoff $\exp(u^\top X_{t+m})$ at time $t+m$ is given by the price-generating function, $\Gamma(u,t,m)$,

$$\begin{aligned}\Gamma(u,t,m) &= E_t\left[M_{t,t+m}\exp\left(u^\top X_{t+m}\right)\right]\\ &= E_t\left[M_{t+1}\Gamma(u,t+1,m-1)\right],\end{aligned}$$

for $u\in\mathbb{R}^4$, where $M_{t,t+i}\equiv M_{t+1}\cdots M_{t+i}$, $M_{t,t+1}=M_{t+1}$ and by convention $M_{t,t}=1$. The price-generating function has the following exponential-affine solution,

$$\Gamma(u,t,m)=\exp\left(c_0(u,t,m)+c(u,t,m)^\top X_t\right), \tag{29}$$

where coefficients satisfy

$$\begin{aligned}c_0(u,t,m) &= c_0(u,t+1,m-1)+A^Q(I_{t+1},c(u,t+1,m-1)))\\ c(u,t,m) &= B^Q(I_{t+1},c(u,t+1,m-1)),\end{aligned} \tag{30}$$

and I_t is an indicator function equal to 1 if an FOMC meeting is scheduled at $t+1$ and 0 otherwise. Initial conditions $c_0(u,t,0)=0$ and $c(u,t,0)=u$ are given by $\Gamma(u,t,0)=\exp(u^\top X_t)$.

Consider the price at time-t of the payoff $\exp(u^\top X_{t+m})$ at maturity m,

$$\begin{aligned}\Gamma(u,t,m) &= E_t\left[M_{t,t+m}\exp\left(u^\top X_{t+m}\right)\right]\\ &= E_t\left[M_{t+1}\Gamma\left(u,t+1,m-1\right)\right].\end{aligned}$$

Substituting the guess $\Gamma(u,t,m)=\exp\left(c_0(u,t,m)+c(u,t,m)^\top X_t\right)$ gives

$$\begin{aligned}\Gamma(u,t,m) =& E_t\left[M_{t+1}\exp\left(c_0(u,t+1,m-1)+c(u,t+1,m-1)^\top X_{t+1}\right)\right]\\ =& \exp\left(c_0(u,t+1,m-1)+A^Q(I_{t+1},c(u,t+1,m-1))\right)\\ &\times\exp\left(\left[B^Q(I_{t+1},c(u,t+1,m-1))-C_r\right]^\top X_t\right),\end{aligned}$$

which implies the following recursion that coefficients must solve:

$$\begin{aligned}c_0(u,t,h) &= c_0(u,t+1,h-1)+A^Q(I_{t+1},c(u,t+1,h-1))\\ c(u,t,h) &= B^Q(I_{t+1},c(u,t+1,h-1))-C_r,\end{aligned}$$

for $0 \leq h \leq m$. Note that $\Gamma(u,t,0) = \exp(u^\top X_t)$ implies $c_0(u,t,0) = 0$ and $c(u,t,0) = u$ for arbitrary $t \geq 1$ and u.

B.2 Discount Bonds

The case $u = 0$ corresponds to the price $D(t,m)$ of a risk-free discount bond with maturity m,

$$D^{rf}(t,m) \equiv \Gamma(0,t,m) = E_t[M_{t,t+m}] = \exp\left(d_0^{rf}(t,m) + d^{rf}(t,m)^\top X_t\right),$$

where $d_0^{rf}(t,m) \equiv c_0(0,t,m)$ and $d^{rf}(t,m) \equiv c(0,t,m)$.

B.3 LIBOR loan

A LIBOR loan is an asset with unit payoff that is further discounted at the rate l_t to offer compensation for illiquidity or counterparty risk. The price of a LIBOR loan can also be obtained from the price-generating function by noting that

$$D^L(t,m) = E_t\left[M_{t,t+m}\exp\left(-\sum_{i=0}^{m-1} l_{t+i}\right)\right] = E_t\left[M^L_{t,t+m}\right],$$

with $M^L_{t+i} = M_{t+i}\exp(-l_{t+1})$. I guess and verify that the solution is exponential-affine, $D^L(t,m) = \exp\left(d_0^L(t,m) + d^L(t,m)^\top X_t\right)$ with solution

$$\begin{aligned} d_0^L(t,m) &= d_0^L(t+1,m-1) + A^Q\left(I_{t+1}, d^L(t+1,m-1)\right) \\ d^L(t,m) &= B^Q\left(I_{t+1}, d^L(t+1,m-1)\right) - C_L, \end{aligned}$$

where $C_L = [1\ 1\ 0\ 1]^\top$. Finally, note that $D^L(t,0) = 1$ implies that $d_0^L(t,0) = 0$ and $d^L(t,0) = 0$ for any $t \geq 1$.

B.4 Singleton Futures Price

A difficulty arises when computing a singleton futures rate because the reference date $t+m$, at which the payoff is determined, is not generally the same as the settlement date $t+T$, at which the payment is made. That is, we have

$$\begin{aligned} f(t,m,T) &= E_t[M_{t,t+T} r_{t+m}] = \\ &= \frac{\partial}{\partial u} E_t\left[M_{t,T}\exp(u r_{t+m})\right]\Big|_{u=0} \equiv \frac{\partial}{\partial u}\Gamma_f(u,t,m,T)\Big|_{u=0}, \end{aligned}$$

where $m \leq T$ and $u \in \mathbb{R}$. However, we can use the law of iterated expectations to obtain

$$\begin{aligned} \Gamma_f(u,t,m,T) &= E_t\left[M_{t,t+m}\exp(u r_{t+m}) E_{t+m}\left[M_{t+m,t+T}\right]\right] \\ &= E_t\left[M_{t,t+m}\exp(u r_{t+m}) D(t+m,T-m)\right] \\ &= \exp(d_0^{rf}(t+m,T-m))\Gamma(d^{rf}(t+m,T-m) + uC_r, t, m). \end{aligned}$$

We can then use the results above to obtain

$$\begin{aligned} &\Gamma_f(u,t,m,T) = \exp\left(d_0^{rf}(t+m,T-m)\right) \\ &\times \exp\left(c_0(d^{rf}(t+m,T-m) + uC_r, t, m) + c(d^{rf}(t+m,T-m) + uC_r, t, m)^\top X_t\right). \end{aligned}$$

Taking the partial derivatives with respect to u and evaluating at $u = 0$, the singleton futures rate is

$$f(t, m, T) = \exp\left(d_0^{rf}(t + m, T - m) + c_0(u^*, t, m) + c(u^*, t, m)^\top X_t\right) \times \left[c_0'(u^*, t, m) + X_t^\top c'(u^*, t, m)\right] C_r,$$

where $u^* = d^{rf}(t + m, T - m)$. The differentiated coefficients, $c_0'(\cdot)$ and $c'(\cdot)$, can be computed by taking derivatives with respect to u on both sides of Equation 30,

$$c_0'(u, t, h) = c_0'(u, t + 1, h - 1) + A'^{Q}(I_{t+1}, c(u, t + 1, h - 1) + \delta)\, c'(u, t + 1, h - 1)$$
$$c'(u, t, h) = B'^{Q}(I_{t+1}, c(u, t + 1, h - 1))\, c'(u, t + 1, h - 1)$$

for any u, t and any $h > 0$. Initial conditions for these differentiated recursions can be found by differentiation of the corresponding initial conditions or by noting that we must have $f(t, 0, T) = D(t, T)r_t$. This yields $c_0'(u, t, 0) = 0$ and $c'(u, t, 0)$ is the identity matrix for any t. Finally, the derivatives of Laplace coefficients $A'^{Q}(\cdot)$ and $B'^{Q}(\cdot)$ can be computed directly.

B.5 Computing Recursions

The recursions in Equation 30 have time and maturity dimensions because the FOMC meeting schedule changes over time. Future meetings get closer by one day every day. At first, it would seem that a different recursion must be computed to match each (t, m) pair, implying a dramatic increase in computing costs. Fortunately, there is a way around this. The key is to note that future meeting dates are known in advance and, therefore, that coefficients $A(\cdot)$ and $B(\cdot)$ are not stochastic. Then, for a given date, and for given parameter values, we can compute coefficients for the price of an asset maturing on this date but also for past observation dates[28] since the recursions are increasing in m but decreasing in t. As an example, consider the price, at some date $t + h$, of an asset maturing on that day. Its price is $\exp(u^\top X_{t+h})$, and the coefficients, $c_0(u, t + h, 0)$ and $c(u, t + h, 0)$ correspond to the initial values in the recursions. Next, consider the price of that asset on the previous day. Its maturity is now 1 and the coefficients, $c_0(u, t+h-1, 1)$ and $c(u, t+h-1, 1)$, are given directly from the recursions above. We can then work our way back until we reach t, the first date in the sample where an asset matures at time $t + h$. Finally, varying the maturity date, t, provides us with all the needed coefficients.[29] In the case of the singleton futures rates, u^* is only a function of the reference date for the singleton futures, $t + h$, and the length of time between the reference date and the settlement date, which will not change as we vary t or m in the coefficient recursions. That is, for a given set of risk-free zero coupon coefficients, we can apply the same strategy as for simple interest rates to compute futures coefficients.

[28] Another approach that reduces computing cost is to assume a constant time interval between meetings beyond the nearest schedule meeting date, as in Piazzesi (2005a). However, the use of federal funds futures contracts makes this approximation problematic as it may place some future meetings in the wrong month, implying severe mispricing of the corresponding futures contracts.

[29] This implies that some recursions must be started for some date $t + h$ beyond the end of the sample. Coefficients are discarded as we proceed backward in time until we reach the last observation date of the sample.

C Estimation

C.1 Data

The Fed targets the overnight fed funds rate. The effective rate is published by the Board of Governors of the Federal Reserve System (see statistical release H.15). It is the weighted average of rates on brokered unsecured federal funds overnight loans between large banks. The payoff of a futures contract depends on the effective rates in a given reference period. Quoted LIBOR rates are annualized (actual/360) but not compounded. I compute the actual day count to maturity using the British banker's association (BBA) Modified ISDA Business Days convention. Futures rates are computed from quoted prices as $F(t,n) = (100 - P(t,n))/3600$ following the Chicago Mercantile Exchange (CME) convention. Each rate is converted to a continuously compounded daily rate. I use the CME "Following Business Days" convention to determine the monthly settlement date. I use end-of-the-day target and effective overnight rates from the Federal Reserve Bank of New York and futures rates from Datastream. LIBOR rates are published around 11h30 by the BBA in London. I match LIBOR data with federal funds and futures rates from the previous day.

C.2 State-Space Representation

The model can be written as a state-space system for the purpose of estimation. The transition equation is given by the VAR representation in Equation 11. The VAR parameters are given by

$$\mu(0)^\top = \begin{bmatrix}\lambda_0^u - \lambda_0^d & \mu_s & \mu_z & \mu_l\end{bmatrix} \qquad \mu(1)^\top = \begin{bmatrix}0 & \mu_s & \mu_z & \mu_l\end{bmatrix}$$

$$\Phi(0) = \begin{bmatrix} 1 & 0 & 0 & 0 \\ \phi_{s,r} & \phi_s & \phi_{s,z} & \phi_{s,l} \\ \phi_{z,r} & \phi_{z,s} & \phi_z & \phi_{z,l} \\ \phi_{l,r} & \phi_{l,s} & \phi l, z & \phi_l \end{bmatrix} \qquad \Phi(1) = \begin{bmatrix} \phi_r(1) & \phi_{r,s}(1) & \phi_{r,z}(1) & \phi_{r,l}(1) \\ \phi_{s,r} & \phi_s & \phi_{s,z} & \phi_{s,l} \\ \phi_{z,r} & \phi_{z,s} & \phi_z & \phi_{z,l} \\ \phi_{l,r} & \phi_{l,s} & \phi l, z & \phi_l \end{bmatrix},$$

where the first row in $\Phi(1)$ can be read from Equation 3.

The measurement equations include LIBOR rates and futures rates, stacked in vector Y_t, and is given by

$$Y_t = \Upsilon(t, X_t) + \epsilon_t, \tag{31}$$

where $\Upsilon(\cdot,\cdot)$ is the model-implied rates and $\epsilon_{i,t}$ are i.i.d. mean zero Gaussian pricing errors with standard deviation ω_i. The measurement equations $\Upsilon(t, X_t)$ combine the solution for LIBOR rates $-\frac{1}{m}\log(D^l(t,m))$ with $D^l(t,m)$ given in Equation 8. The measurement equations also include futures rates given in Proposition 1, as well as the target rate and the effective spread, stacked together with yields in the vector $\tilde{Y}_t = [r_t \; s_t \; Y_t]^\top$.

C.3 Unscented Kalman Filter

The state variables z_t and l_t are latent and are filtered from the data using the UKF. The Kalman filter is not applicable since futures rates are nonlinear functions of the states and, moreover, the optimal filter is not available in closed form. The UKF provides an approximation to nonlinear transformations of a probability distribution. It has a Monte Carlo flavor but the sample is drawn according to a deterministic algorithm. It reduces the computational burden considerably, relative to simulation-based methods, but provides greater accuracy than linearization (Christoffersen et al., 2014). The UKF has been introduced in Julier et al. (1995) and Julier and Uhlmann (1996) (see Wan and der Merwe 2001, for textbook treatment) and was first imported to finance by Leippold and Wu (2003).

Given $\hat{X}_{t+1|t}$ a time-t forecast of X_{t+1}, and its associated RMSE, $\hat{Q}_{t+1|t}$, the filter selects a set of sigma points in the distribution of $X_{t+1|t}$ such that

$$\bar{\mathbf{x}} = \sum_i w^{(i)} x^{(i)} = \hat{X}_{t+1|t} \quad \text{and} \quad \mathbf{Q}_x = \sum_i w^{(i)} (x^{(i)} - \bar{\mathbf{x}})(x^{(i)} - \bar{\mathbf{x}})' = \hat{Q}_{t+1|t}.$$

Julier et al. (1995) proposed the following set of sigma points and weights:

$$x^{(i)} = \begin{cases} \bar{\mathbf{x}} & i = 0 \\ \bar{\mathbf{x}} + \left(\sqrt{\frac{N_x}{1-w^{(0)}} \sum_x}\right)_{(i)} & i = 1, \ldots, K \\ \bar{\mathbf{x}} - \left(\sqrt{\frac{N_x}{1-w^{(0)}} \sum_x}\right)_{(i-K)} & i = K+1, \ldots, 2K \end{cases} \qquad w^{(i)} = \begin{cases} w^{(0)} & i = 0 \\ \frac{1-w^{(0)}}{2K} & i = 1, \ldots, K \\ \frac{1-w^{(0)}}{2K} & i = K+1, \ldots, 2K \end{cases},$$

where $\left(\sqrt{\frac{N_x}{1-w^{(0)}} \sum_x}\right)_{(i)}$ is the i-th row or column of the matrix square root. Julier and Uhlmann (1996) use a Taylor expansion to evaluate the approximation's accuracy. The expansion of $y = g(x)$ around $\bar{x}$ is

$$\bar{y} = E\left[g(\bar{x} + \Delta x)\right] = g(\bar{x}) + E\left[D_{\Delta x}(g) + \frac{D^2_{\Delta x}(g)}{2!} + \frac{D^3_{\Delta x}(g)}{3!} + \cdots\right],$$

where the $D^i_{\Delta x}(g)$ operator evaluates the total differential of $g(\cdot)$ when perturbed by Δx, and evaluated at $\bar{x}$. A useful representation of this operator in our context is

$$\frac{D^i_{\Delta x}(g)}{i!} = \frac{1}{i!} \left(\sum_{j=1}^{n} \Delta x_j \frac{\partial}{\partial x_j}\right)^i g(x)\Big|_{x=\bar{x}}.$$

Different approximation strategies for $\bar{y}$ will differ by either the number of terms used in the expansion or the set of perturbations Δx. If the distribution of Δx is symmetric, all odd-ordered terms are 0 and we can rewrite the second term as a function of the covariance matrix P_{xx} of Δx,

$$\bar{y} = g(\bar{x}) + \left(\nabla^\top P_{xx} \nabla\right) g(\bar{x}) + E\left[\frac{D^4_{\Delta x}(g)}{4!} + \cdots\right].$$

Linearization leads to the approximation $\hat{\bar{y}}_{lin} = g(\bar{x})$, while the unscented approximation is exact up to the third-order term. In the Gaussian case, Julier and Uhlmann (1996) show that same-variable fourth moments agree as well and that all other moments are lower than the true moments of Δx. Then, approximation errors of higher-order terms are necessarily smaller for the UKF than for the extended Kalman filter. Using a similar argument, Julier and Uhlmann (1996) show that linearization and the unscented transformation agree with the Taylor expansion up to the second-order term and that approximation errors in higher-order terms are smaller for the UKF.

C.4 Identification Assumption

The following identification restrictions were imposed on the parameter space. First, $\mu_z = 0$ to identify the level of z_{t+1} separately from that of $\lambda_{z,u}$ and $\lambda_{z,d}$. Second, $\lambda_{z,u} > 0$ and $\lambda_{z,d} > 0$ to identify the sign of z_{t+1}. The following restrictions are imposed for stationarity. The eigenvalues of the matrix $\Phi(I_{t+1} = 1)$ must lie within the unit circle. First, $\lambda_{u,r} < 0$ and $\lambda_{d,r} < 0$ so that $\phi_r(1) < 1$ and the policy function induces reversion to the mean, since $\phi_{s,r} = \phi_{z,r} = \phi_{l,r} = 0$. Intuitively, if s_t, z_t and l_t are jointly stationary, then mean-reversion follows if the intensity of an "up" change

decreases and the intensity of a "down" change increases when the target rate increases. Table 5 reports all parameter estimates. Joint stationarity follows if s_t, z_t and l_t are jointly stationary. The following re-parameterization is used:

$$\tilde{\phi} = [I - \phi]^{-1} = \left[I - \begin{bmatrix} \phi_z & \phi_{z,l} \\ \phi_{l,z} & \phi_l \end{bmatrix} \right]^{-1}, \tag{32}$$

where $\tilde{\phi}$ must be invertible. Finally, $|\phi_s| < 1$.

The jump component of the effective rate is well defined only if $\lambda_{J,s} \geq 0$. I impose that $\lambda_{z,d} \geq 0$ and $\lambda_{z,u} \geq 0$ to identify the sign of z_t. More importantly, λ_t^u and λ_t^d must remain non-negative so that the distribution of target jumps remains well defined. These constraints cannot be easily imposed on the parameter space as they can be checked recursively as we filter the state variables. In practice I impose that $\hat{\lambda}_t^i = \max\left(0, \lambda_t^i\right)$. This leaves state variables unrestricted but constrains the policy function. The restriction is reasonable. As λ_t^i approaches 0, the probability distribution of the corresponding jump n_t^i approaches the trivial distribution with a unit mass at 0. When it reaches 0, the policy function becomes one-sided and can then be summarized as a Poisson distribution. The constrained quasi maximum likelihood estimator is given by

$$\hat{\Theta}^{QML} = \underset{\Theta}{\operatorname{argmax}}\ L(\theta; Y) \quad s.t. \quad \Theta \in S$$

where $S \subseteq \mathbb{R}^K$and we have $\hat{\Theta} \sim N(\Theta_0, T^{-1}\Omega)$ for some true parameter value, Θ_0, in the interior of the parameter space. Optimization of the log-likelihood is carried out using the active-set algorithm from the IMSL Fortran optimization library. I report estimates for $\hat{\phi} = I - \hat{\tilde{\Phi}}^{-1}$ and the p-values associated with Wald statistics computed for the nulls that each individual coefficient is 0.

D Predictability Coefficients

D.1 Multi-Horizon Laplace Transform

The distribution of future state variables can be characterized explicitly from the multi-horizon conditional Laplace transform,

$$T_X(u, t, h) \equiv E_t \left[\exp(u^\top X_{t+h}) \right],$$

for any $u \in \mathbb{R}^K$ and $h \geq 1$. The solution is exponential affine,

$$T_X(u, t, h) \equiv E_t \left[T_X(u, t+1, h-1) \right] = \exp\left(A(I_{t+1}, z, h) + B(I_{t+1}, z, h)^\top X_t \right),$$

with coefficients given by

$$\begin{aligned} A(I_t, z, h+1) =& A(I_{t+1}, z, h) + A(I_t, B(I_{t+1}, z, h)) \\ B(I_t, z, h+1) =& B(I_t, B(I_{t+1}, z, h)), \end{aligned}$$

for any $h \geq 1$ with initial conditions $A(I_{t+1}, z, 1) = A(I_{t+1}, z)$ and $B(I_{t+1}, z, 1) = B(I_{t+1}, z)$.

D.2 Conditional Expectations

The conditional expectation of linear combinations of the state variables $C^\top X_t$ can be derived at any horizon from the following partial derivative with respect to u,

$$\begin{aligned} E_t\left[C^\top X_{t+h}\right] &= \left[\frac{\partial}{\partial u} T_X(uC,t,h)\right]_{u=0} \\ &= \left[T_X(uC,t,h)\left(A_2'(I_{t+1},uC,h) + X_t^\top B_2'(I_{t+1},uC,h)\right)C\right]_{u=0} \\ &= \left(A_2'(I_{t+1},0,h) + X_t' B_2^\top(I_{t+1},0,h)\right)C, \end{aligned}$$

where, as before, the derivatives of the multi-horizon coefficients can be obtained by differentiating their respective recursions and

$$\begin{aligned} A_2^\top(I_{t+1},0,h) =& A_2^\top(I_{t+2},0,h-1) + A_2^\top(I_{t+1},B(I_{t+2},0,h-1))B_2^\top(I_{t+2},0,h-1)) \\ B_2^\top(I_{t+1},0,h)) =& B_2^\top(I_{t+2},B(I_{t+2},0,h-1))B_2^\top(I_{t+2},0,h-1)), \end{aligned}$$

with initial conditions $A_2^\top(I_{t+1},0,1) = A_2^\top(I_{t+1},0)$ and $B_2^\top(I_{t+1},0,1) = B_2^\top(I_{t+1},0)$.

D.3 Forecasting Federal Funds Rates

The forecasts of target and effective overnight federal funds rates can by computed by setting $C = C_r = [1\ 0\ 0\ 0]^\top$ and $C = C_{r+s} = [1\ 1\ 0\ 0]^\top$, respectively. We have,

$$\begin{aligned} E[r_{t+h}|X_t = x] =& a_r(I_{t+1},h) + b_r(I_{t+1},h)^\top X_t \\ E[r_{t+h}|X_t = x] =& a_{r+s}(I_{t+1},h) + b_{r+s}(I_{t+1},h)^\top X_t. \end{aligned}$$

Figure 1: Forward LIBOR and Futures Rates

LIBOR forward rates and futures rates at maturities of two, four and six months. Daily data from January 1994 to July 2007.

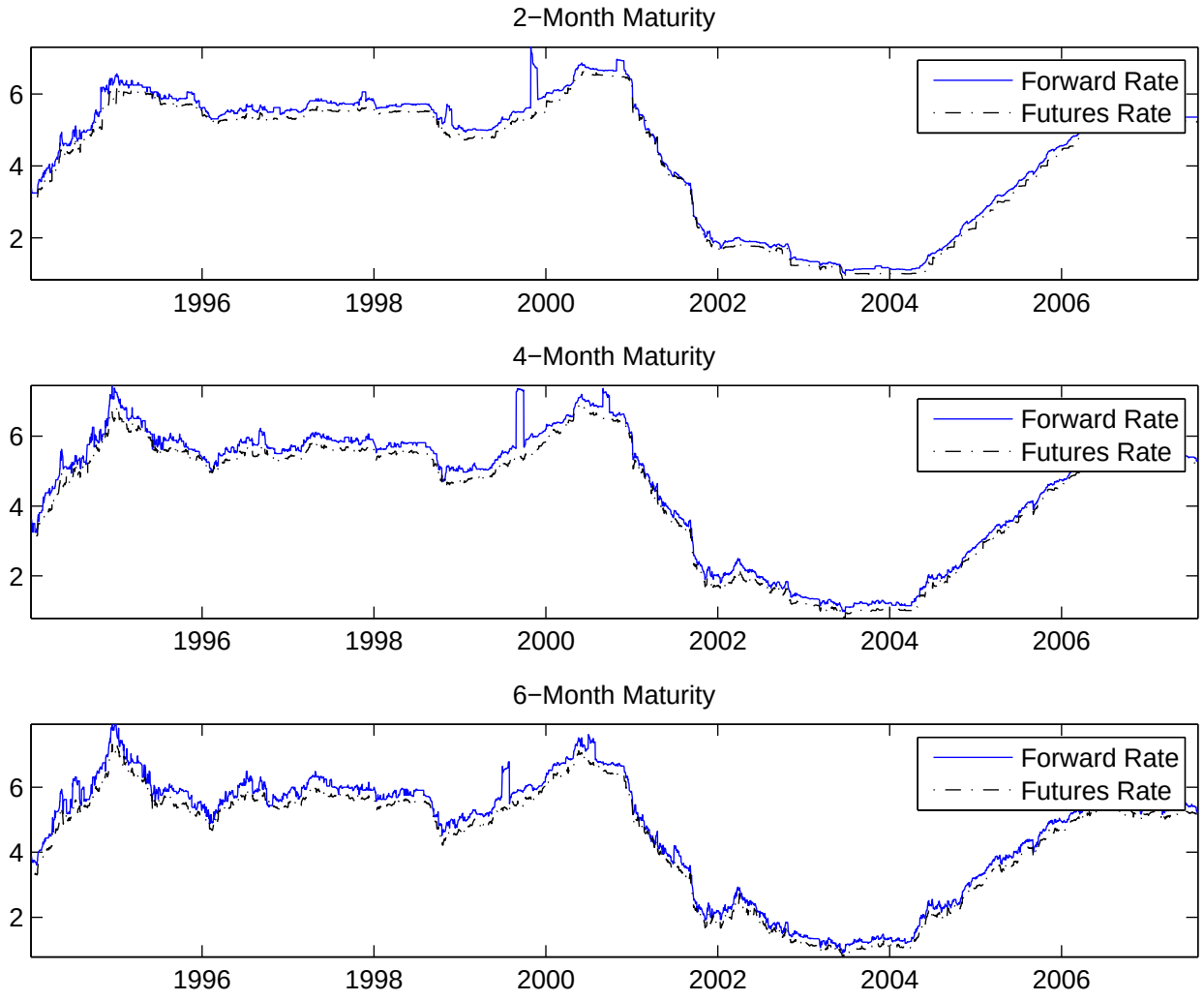

Figure 2: Target Rate, the Path Factor and Economic Conditions

Target rate, the path factor, the spread factor and the ADS index of real activity. Panel (a) displays the path factor and the target rate. Panel (b) displays the ADS index and the target rate. Panel (c) displays the path and spread factors. Factors are from QML estimation of the model. ADS index is from the Philadelphia Federal Reserve Bank's website.

(a) Target Rate and Path Factor

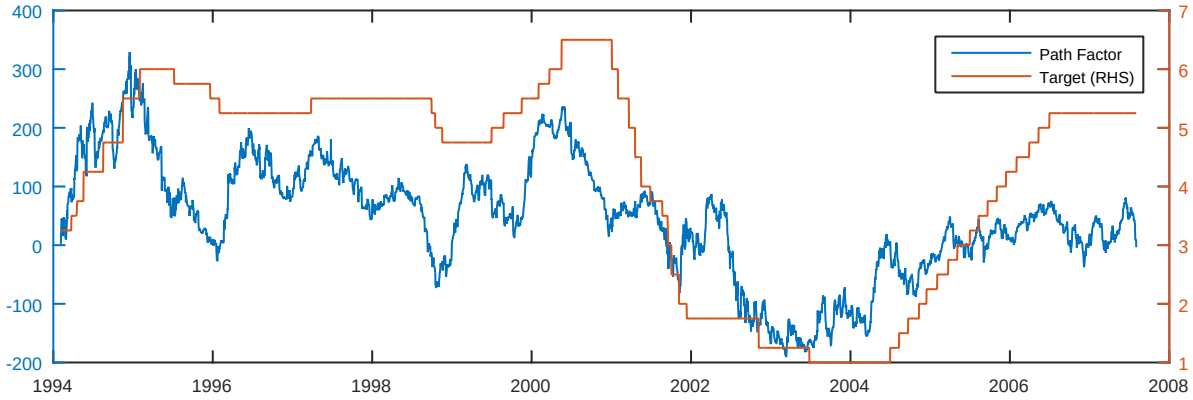

(b) ADS Index and Path Factor

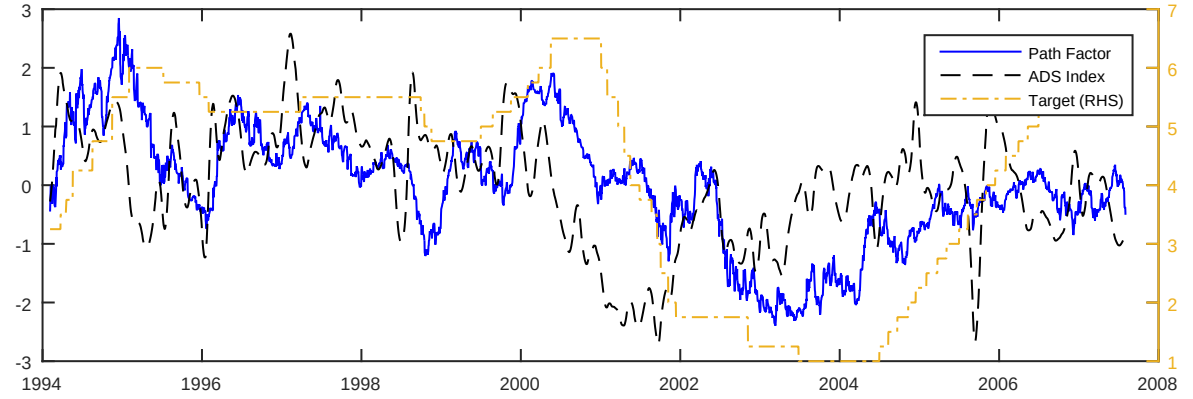

(c) Liquidity and Path Factor

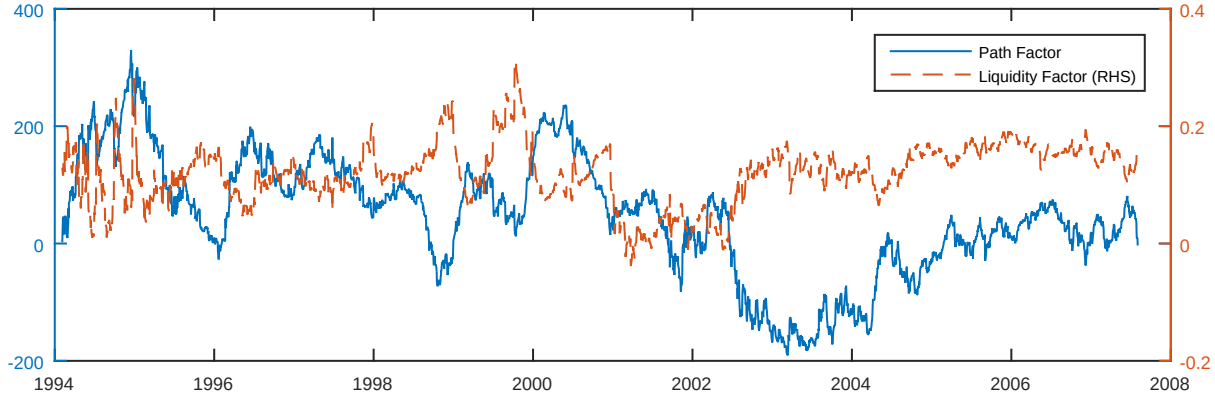

Figure 3: Conditional Moments of Target Rate Changes and State Variables

Variations of the target rate conditional distribution across values of state variables. In Panels (a) and (b), the sample is divided in three subsample along the terciles of the path factor. Each subsample is then divided along its own target rate tercile. There are nine subsamples. Panel (a) displays conditional variance in each subsample, Panel (b) displays conditional skewness. In Panel (c) the risk premium for a 6-month federal funds futures. In this case, the sample is divided into 9 subsamples using the target rate and the level of conditional volatility. Moments are computed using Equation (a)-(b) and reflect the distribution of the FOMC decision measured on a day preceding a scheduled FOMC meeting. Conditional volatility is measured in annualized percentage, skewness is unitless and the risk premium is measured in bps (annualized).

(a) Conditional Volatility

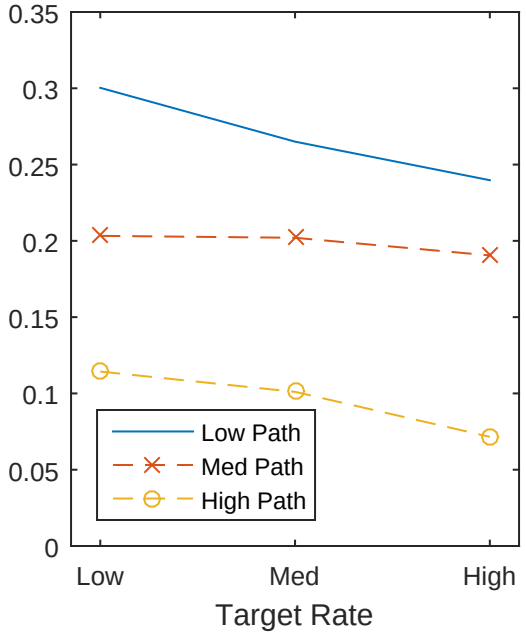

(b) Conditional Skewness

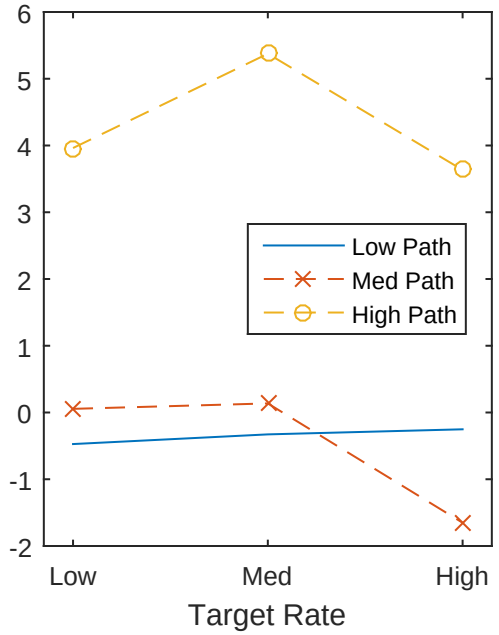

(c) Risk Premium on Futures

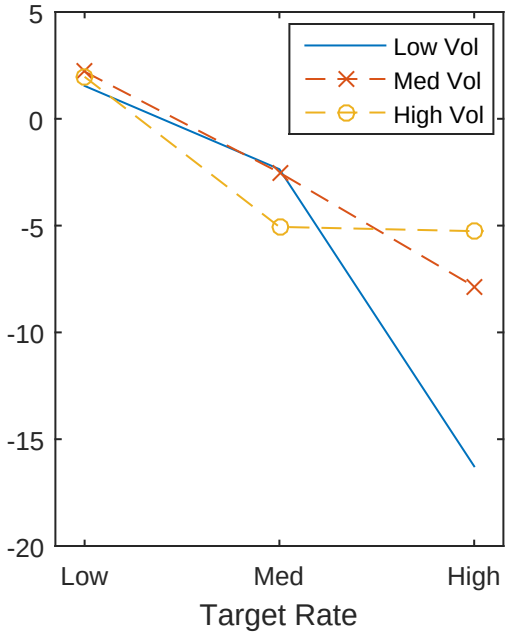

Figure 4: Conditional Distribution of Target Rate Changes

The target rate conditional distributions across values of state variables. The sample is divided along the terciles of the path factor. Each subsample is then divided along its own target rate terciles. There are nine subsamples. Panel 4(a) displays the conditional distribution of target changes for the average values of state variables in the (*low*, *low*) subsample, Panel 4(b) in the (*med*, *med*) subsample and Panel 4(c) in the (*high*, *high*) subsample. Conditional probabilities reflect the distribution measured on a day preceding a scheduled FOMC meeting.

(a) Low Path Factor and Target Rate

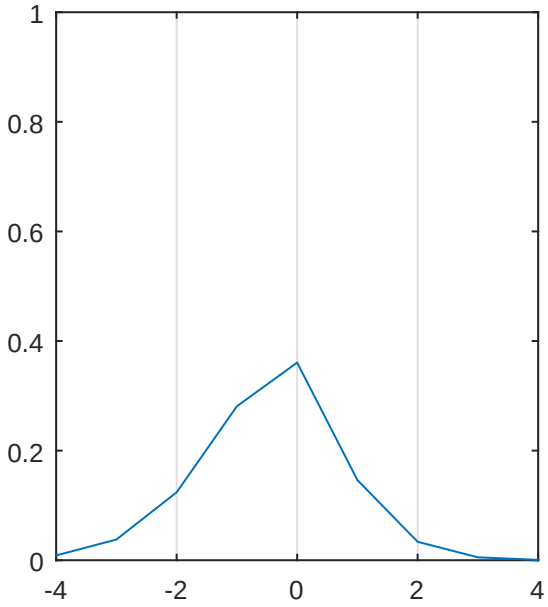

(b) Median Path Factor and Target Rate

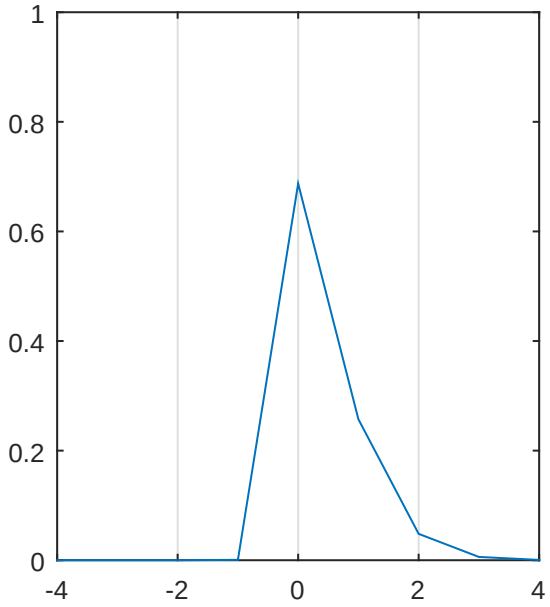

(c) High Path Factor and Target Rate

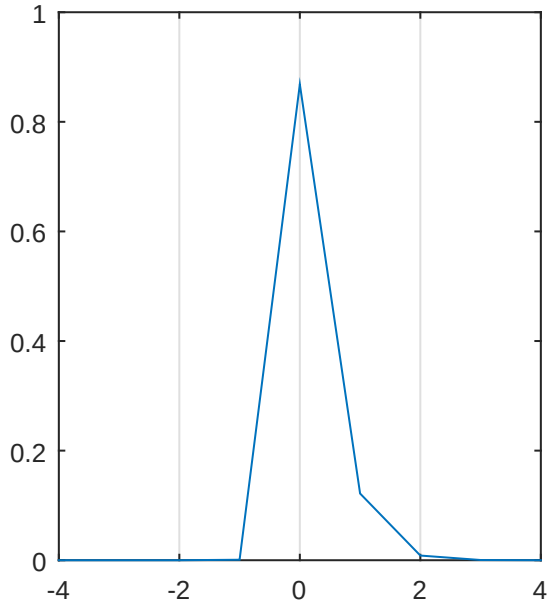

Figure 5: Forecasting Target Rates: RMSE and R^2s

RMSE and R^2 from predictive regressions of monthly target rate average, $\bar{r}_n$ at daily horizons up to 12 months. The predictive regressions are given by

$$\begin{aligned} E_t[\bar{r}_n] =& \bar{a}(t,n) + \bar{b}(t,n)^T X_t \\ E_t^{fut}[\bar{r}_n] =& \alpha_h^{fut} + \beta_h^{fut} F(t,n) \\ E_t^{lib}[\bar{r}_n] =& \alpha_h^{lib} + \beta_h^{lib} F_{lib}(t,n), \end{aligned}$$

where $\bar{a}(t,n)$ and $\bar{b}(t,n)$ are model-implied coefficients for a time-t forecast of the average effective rate in calendar month n, $\bar{r}_n$, so that h is the number of days between t and the end of month n. $F(t,n)$ and $F_{lib}(t,n)$ are the observed futures and forward LIBOR rates corresponding to calendar month n at time-t. Panel (a) compares the RMSE in percentage (annualized) and the x-axis is the horizon, h, from 1 to 360 days ahead. Panel (b) compares R^2.

(a) RMSE

(b) R^2

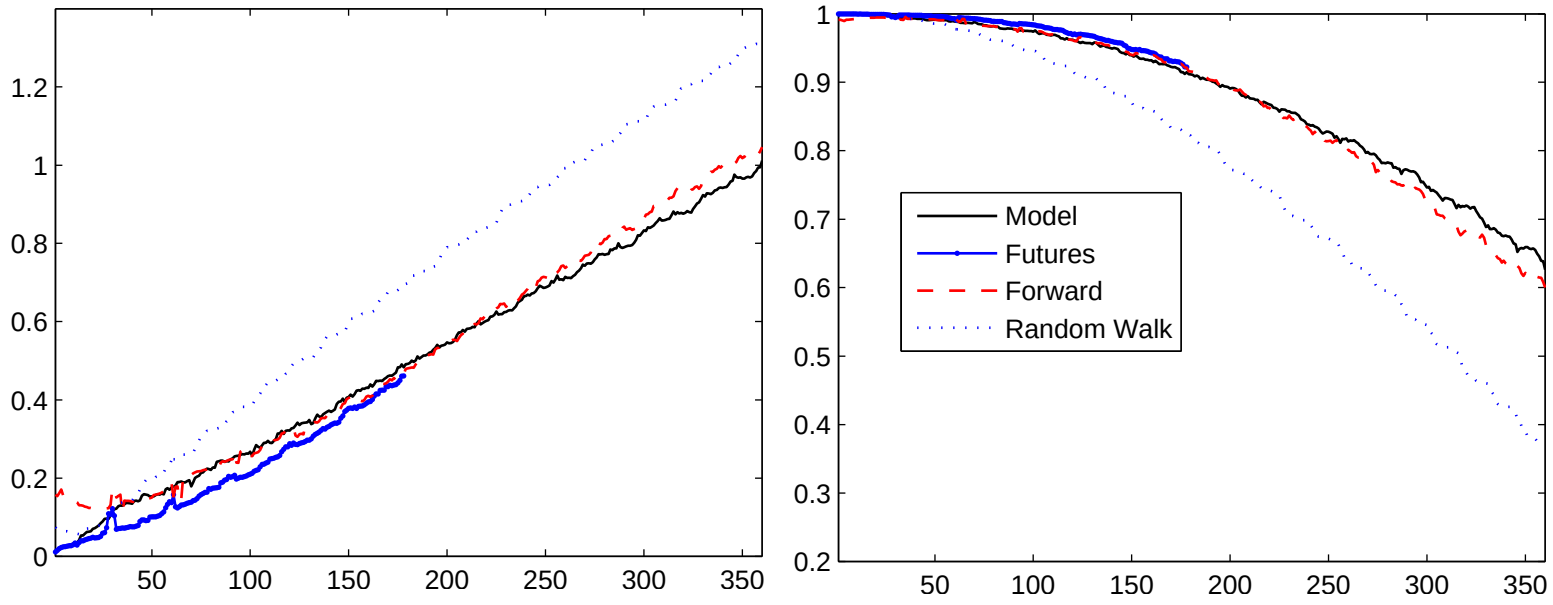

Figure 6: Forecasting Target Rates: Forecast Errors

Forecast errors from predictive regressions of monthly target rate average, $\bar{r}_n$ at daily horizons up to 12 months. The predictive regressions are given by

$$\begin{aligned} E_t[\bar{r}_n] =& \bar{a}(t,n) + \bar{b}(t,n)^T X_t \\ E_t^{fut}[\bar{r}_n] =& \alpha_h^{fut} + \beta_h^{fut} F(t,n) \\ E_t^{lib}[\bar{r}_n] =& \alpha_h^{lib} + \beta_h^{lib} F_{lib}(t,n), \end{aligned}$$

where $\bar{a}(t,n)$ and $\bar{b}(t,n)$ are model-implied coefficients for a time-t forecast of the average effective rate in calendar month n, $\bar{r}_n$, so that h is the number of days between t and the end of month n. $F(t,n)$ and $F_{lib}(t,n)$ are the observed futures and forward LIBOR rates corresponding to calendar month n at time-t. For each observation day, Panel (a) shows the average forecast errors at horizons between 90 and 180 days, Panel (b) at horizons between 180 and 270 days and Panel (c) at horizons between 180 and 270 days.

(a) Horizons from 90 to 180 days

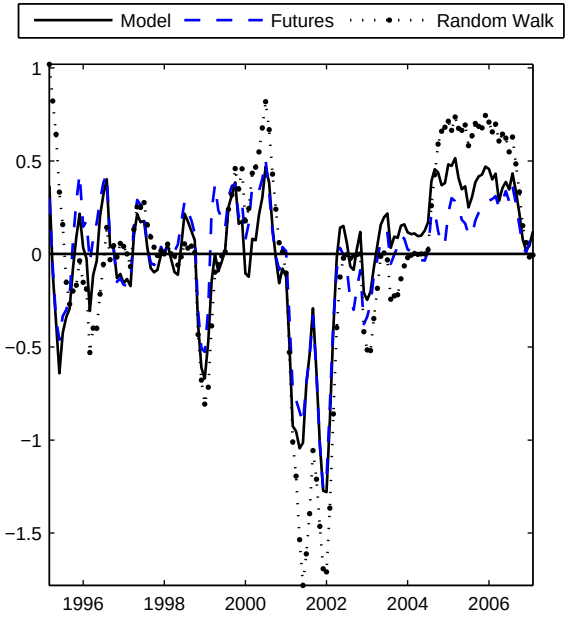

(b) Horizons from 180 to 270 days

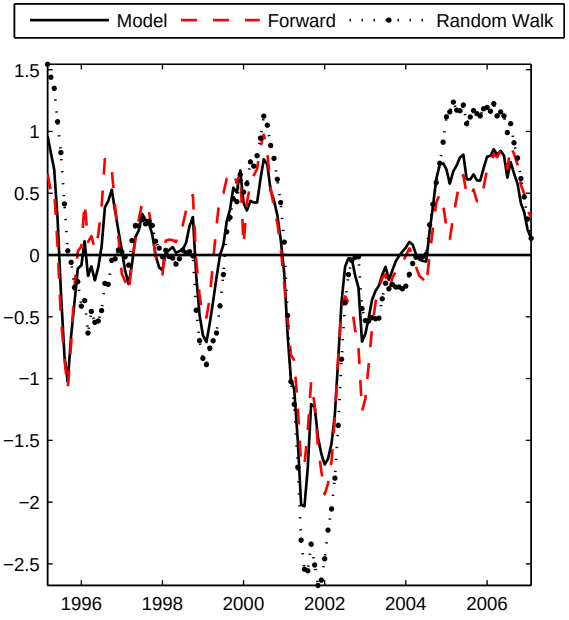

(c) Horizons from 270 days to 360 days

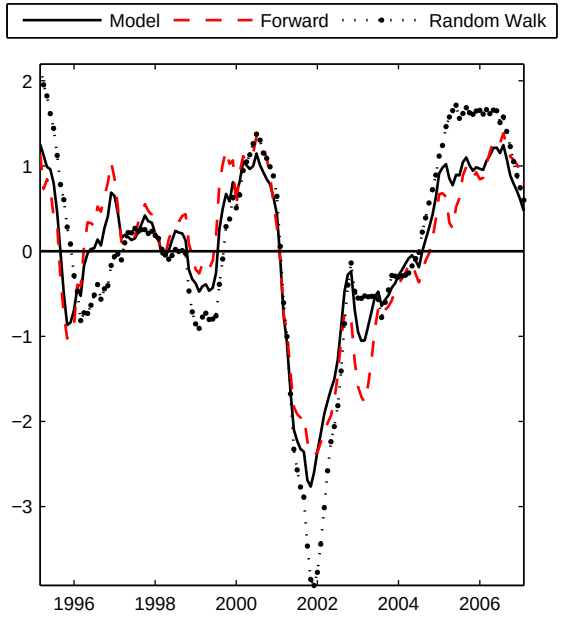

Figure 7: Risk Premium

Panel (a) compares the risk premium predicted by the model for the six-month-ahead contract with the subsequent realized returns on that contract.

(a) Risk Premium and Excess Returns

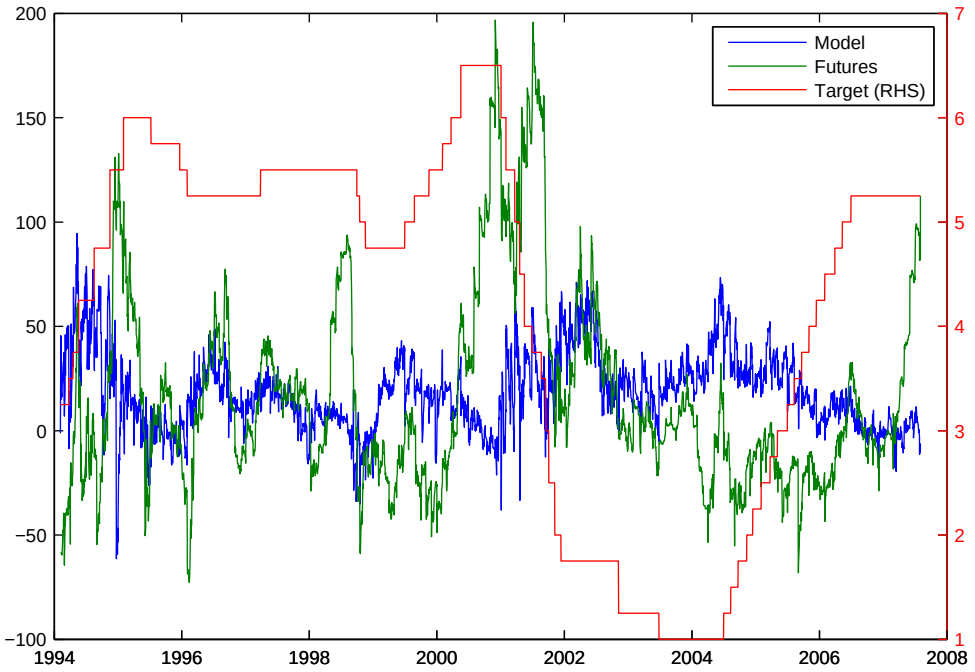

Table 1: **LIBOR Rates Summary Statistics**

Means μ_i and standard deviations σ_i of simple annualized LIBOR rates. Panel 1(a): LIBOR rates. Panel (b): forward LIBOR rates. Panel (c): futures rates. Panel (d): spreads between futures and forward rates. LIBOR and forward rates with maturities from 1 to 12 months. Futures for horizons of 1 to 6 months. Daily data from 3 January 1994 to 31 July 2007.

(a) LIBOR Rates

	Maturity (month)											
	1	2	3	4	5	6	7	8	9	10	11	12
μ_{Lib}	4.33	4.37	4.41	4.44	4.47	4.50	4.54	4.57	4.60	4.63	4.67	4.70
σ_{Lib}	1.76	1.77	1.78	1.78	1.78	1.78	1.78	1.78	1.78	1.77	1.77	1.77

(b) Forward Rates

	Maturity (month)											
	1	2	3	4	5	6	7	8	9	10	11	12
μ_{For}	4.33	4.41	4.49	4.54	4.61	4.66	4.73	4.79	4.84	4.95	5.01	5.07
σ_{For}	1.76	1.78	1.80	1.80	1.80	1.80	1.79	1.79	1.79	1.78	1.77	1.74

(c) Futures Rates

	Maturity (month)					
	1	2	3	4	5	6
μ_{Fut}	4.18	4.21	4.25	4.28	4.33	4.37
σ_{Fut}	1.74	1.75	1.75	1.76	1.76	1.75

(d) Forward-to-Futures Spreads

	Maturity (month)					
	1	2	3	4	5	6
μ_{diff}	0.14	0.20	0.24	0.25	0.28	0.29
σ_{diff}	0.14	0.15	0.18	0.17	0.17	0.14

Table 2: **Principal Component Analysis of Forward-Futures Spreads**

Principal component analysis of forward-to-futures spreads at monthly maturities from 1 to 6 months. Each column displays the loading across maturities and the contribution to the variance explained for each component. Daily data from 3 January 1994 to 31 July 2007, but excluding the last nine months of 1999.

	Components Loadings					
Maturity	PC1	PC2	PC3	PC4	PC5	PC6
1	0.44	0.77	-0.05	-0.10	0.29	0.31
2	0.38	0.13	-0.02	0.14	-0.90	-0.00
3	0.42	0.04	0.08	0.24	0.23	-0.83
4	0.37	-0.28	0.18	-0.85	-0.02	-0.06
5	0.37	-0.32	0.65	0.37	0.15	0.39
6	0.43	-0.43	-0.72	0.16	0.16	0.21
R^2	0.53	0.13	0.12	0.09	0.07	0.06
$Cum.R^2$	0.53	0.66	0.77	0.88	0.94	1

Table 3: **Excess Returns and Components from Forward-to-Futures Spreads**

Results from predictive regressions of monthly futures excess returns (Panel (a)) and monthly forward excess returns (Panel (b)):

$$xr_{t,n} = \gamma_{0,n} + \gamma_{lvl}\ level_t + \gamma_{slp}\ slope_t + u_{t,n},$$

where $level_t$ and $slope_t$ are the first two components extracted from forward-to-futures spreads. Regressors are centered on 0 and normalized by their standard deviations. Excess returns are in bps (annualized). I include t-statistics based on Newey–West standard errors (six lags) in parentheses and R^2 in brackets. Monthly data from January 1994 to June 2007.

(a) Futures Excess Returns

	Maturity (month)				
	2	3	4	5	6
γ_0	0.02	0.02	0.03	0.03	0.04
	(2.35)	(1.99)	(2.14)	(1.99)	(1.94)
γ_{lvl}	0.00	-0.03	-0.02	-0.03	-0.02
	(0.15)	(-1.04)	(-1.05)	(-1.15)	(-1.03)
γ_{slp}	0.03	0.05	0.06	0.07	0.07
	(1.41)	(2.78)	(2.84)	(2.93)	(2.83)
R^2	[2.8]	[8.3]	[7.4]	[6.5]	[5.6]

(b) Forward Excess Returns

	Maturity (month)										
	2	3	4	5	6	7	8	9	10	11	12
γ_0	0.08	0.06	0.04	0.08	0.05	0.08	0.07	0.07	0.12	0.07	0.07
	(6.54)	(4.29)	(2.23)	(4.39)	(2.59)	(2.80)	(2.98)	(2.29)	(3.34)	(2.07)	(1.79)
γ_{lvl}	0.03	0.01	-0.02	0.01	-0.00	0.02	0.03	0.04	0.04	0.03	0.01
	(0.91)	(0.55)	(-0.63)	(0.41)	(-0.02)	(0.65)	(1.27)	(1.24)	(1.09)	(0.92)	(0.13)
γ_{slp}	0.05	0.05	0.07	0.09	0.10	0.11	0.10	0.09	0.14	0.11	0.07
	(2.37)	(2.14)	(2.84)	(3.18)	(3.55)	(3.04)	(2.86)	(2.73)	(3.39)	(2.58)	(1.75)
R^2	[5.7]	[3.5]	[6.6]	[5.8]	[7.3]	[6.4]	[4.8]	[4.1]	[5.4]	[4.3]	[1.5]

Table 4: **Pricing Error Statistics**

Mean pricing errors (MPE) and root mean squared pricing errors (RMSE). The sample ranges from January 1994 to July 2007. Results are reported in percentage (annualized), for LIBOR rates and futures rates at maturities of 1 to 12 months and 1 to 6 months, respectively.

(a) MSE (bps $\times 10^{-2}$)

	Maturity (month)											
	1	2	3	4	5	6	7	8	9	10	11	12
LIBOR	-1.35	-0.48	0.27	0.12	0.19	0.05	0.03	-0.03	-0.20	-0.02	0.07	-0.08
Futures	-0.09	0.06	0.23	0.55	0.54	0.09						

(b) RMSE (bps)

	Maturity (month)											
	1	2	3	4	5	6	7	8	9	10	11	12
LIBOR	0.10	0.07	0.06	0.04	0.03	0.01	0.01	0.01	0.01	0.01	0.00	0.01
Futures	0.03	0.06	0.08	0.10	0.11	0.12						

Table 5: **Parameter Estimates**

Parameter estimates from daily data (January 1994 to July 2007). Panel (a) and (b) display parameters for the latent variables and effective spread dynamics, respectively. Panel (c) displays parameter estimates for the policy function. Panel (d) displays price of risk parameters. In each case, standard errors are provided in parenthesis. The estimate for λ is 0.3293 and its standard error is (0.0054). In panel (a), the symbols ** indicates statistical significance at the one percent level, respectively, corresponding to the Wald statistics that individual coefficients are different from 0.

(a) Latent Factor Dynamics

	μ	$\phi_{i,i}$	$\phi_{i,j}$	σ	$\rho_{l,z}$
z_t	0	0.998^{**}	$1.89 \times 10^{-3**}$	7.91^{**}	-0.11^{**}
l_t	$1.03 \times 10^{-3**}$	0.992^{**}	-2.18×10^{-6}	$8.14 \times 10^{-2**}$	-

(b) Effective Spread Dynamics

	$\mu \times 10^{-3}$	ϕ	σ	ν_s	ω_s	λ_s
s_t	-3.54	0.20	0.05	0.69	0.27	0.23
	(0.53)	(0.012)	(0.001)	(0.005)	(0.013)	(0.022)

(c) Policy Function

	$r \times 10^3$	s	$z \times 10^{-3}$	l
λ_u	-104.04	0	4.63	9.05
	(0.055)	-	(0.034)	(0.069)
λ_d	-98.95	0	9.14	8.50
	(0.060)	-	(0.089)	(0.058)

(d) Prices of Risk

	$r \times 10^3$	$s \times 10^3$	$z \times 10^{-3}$	$l \times 10^{-2}$
δ	-7.47	8.90	7.24	4.42
	(0.078)	(0.069)	(0.056)	(0.093)
	$r \times 10^{-2}$	s	$z \times 10^{-6}$	$l \times 10^{-3}$
$\delta_{1,z}$	-2.52	0	-2.91	6.25
	(0.059)	-	(0.080)	(0.054)

Table 6: **Predictive Regressions: Forward vs Futures Excess Returns**

Results from predictive regressions of monthly futures and forward excess returns on the spread factor, l_t. Excess returns are in bps (annualized). Coefficient estimates provide the change in expected excess returns due to a change of one standard deviation in l_t. Newey–West t-statistics (six lags) in parentheses and R^2 in brackets.

(a) $xr^{Fut}_{t,n} = \gamma_{0,n} + \gamma_{l,n} l_t + u_{t,n}$

	Maturity (month)				
	2	3	4	5	6
γ_0	2.20	2.16	2.75	3.02	3.52
	(2.27)	(1.71)	(1.80)	(1.69)	(1.77)
γ_l	-1.38	-3.22	-3.98	-4.94	-5.93
	(-1.03)	(-1.93)	(-1.93)	(-2.16)	(-2.42)
R^2	[1.4]	[5.3]	[5.2]	[5.9]	[6.5]

(b) $xr^{For}_{t,n} = \gamma_{0,n} + \gamma_{l,n} l_t + u_{t,n}$

	Maturity (month)										
	2	3	4	5	6	7	8	9	10	11	12
γ_0	9.97	7.65	5.71	8.15	3.90	11.03	6.91	6.12	15.71	8.14	7.41
	(6.26)	(5.08)	(2.50)	(3.80)	(1.61)	(3.42)	(2.50)	(1.84)	(4.36)	(2.04)	(1.92)
γ_l	-2.80	-1.25	0.05	-0.90	1.92	-1.66	-1.72	1.87	-1.24	-0.65	1.59
	(-2.15)	(-1.03)	(0.03)	(-0.53)	(0.81)	(-0.58)	(-0.72)	(0.69)	(-0.43)	(-0.20)	(0.51)
R^2	[2.3]	[0.4]	[0.0]	[0.1]	[0.6]	[0.3]	[0.4]	[0.3]	[0.1]	[0.0]	[0.1]

Table 7: **Predictive Regressions: The Role of Hedging Demand**

Results from predictive regressions of monthly futures excess returns on different combinations of spread factor, l_t, the path factor, z_t and the net long position by non-commercial investors, NLP_t. Excess returns are in bps (annualized). Coefficient estimates provide the change in expected excess returns due to a change of one standard deviation in the regressors. Newey–West t-statistics (six lags) in parentheses and R^2 in brackets.

(a) $xr_{t,n}^{Fut} = \gamma_{0,n} + \gamma_{nlp} NLP_t + u_{t,n}$

	Maturity (month)				
	2	3	4	5	6
γ_0	2.20	2.16	2.75	3.02	3.52
	(2.20)	(1.59)	(1.70)	(1.61)	(1.71)
γ_{nlp}	1.60	2.84	3.88	4.66	5.64
	(1.17)	(1.61)	(1.96)	(2.13)	(2.43)
R^2	[1.9]	[4.1]	[5.0]	[5.3]	[5.9]

(b) $xr_{t,n}^{Fut} = \gamma_{0,n} + +\gamma_l l_t + \gamma_{nlp} NLP_t u_{t,n}$

	Maturity (month)				
	2	3	4	5	6
γ_0	2.20	2.16	2.75	3.02	3.52
	(2.30)	(1.76)	(1.88)	(1.79)	(1.92)
γ_l	-0.90	-2.50	-2.92	-3.69	-4.41
	(-0.81)	(-1.80)	(-1.57)	(-1.77)	(-1.95)
γ_{nlp}	1.26	1.88	2.75	3.24	3.94
	(1.10)	(1.35)	(1.66)	(1.74)	(1.94)
R^2	[2.4]	[6.8]	[7.4]	[8.1]	[9.0]

(c) $xr_{t,n}^{Fut} = \gamma_{0,n} + \gamma_z z_t + \gamma_l l_t + \gamma_{nlp} NLP_t + u_{t,n}$

	Maturity (month)				
	2	3	4	5	6
γ_0	2.20	2.16	2.75	3.02	3.52
	(2.40)	(1.82)	(1.93)	(1.84)	(1.96)
γ_z	2.30	3.07	3.93	4.77	5.41
	(1.83)	(1.86)	(1.72)	(1.83)	(1.97)
γ_l	0.16	-1.08	-1.11	-1.50	-1.92
	(0.12)	(-0.63)	(-0.47)	(-0.57)	(-0.73)
γ_{nlp}	2.77	3.91	5.35	6.38	7.51
	(2.07)	(2.18)	(2.40)	(2.52)	(2.86)
R^2	[4.7]	[9.7]	[10.4]	[11.3]	[12.2]

Table 8: **Predictive Regressions: Excess Holding Returns**

Results from predictive regressions of futures excess holding returns. Predictors include the path factor, z_t, the spread factor, l_t, and the net position of non-commercial participants, NLP_t. Regressors are centered on 0 and normalized by their standard deviations. Excess returns are in bps (annualized). Coefficient estimates provide the change in expected excess returns due to a change of one standard deviation in the regressors. I include t-statistics based on Newey–West standard errors (six lags) in parentheses and R^2 in brackets.

(a) $xr_{t,n} = \gamma_{0,n} + \gamma_{l,n} l_t + u_{t,n}$

	Maturity (month)					
	2	3	4	5	6	
$\gamma_{0,n}$	0.78	2.91	5.25	8.52	12.32	16.40
	(2.28)	(3.58)	(3.69)	(4.00)	(4.36)	(4.55)
$\gamma_{l,n}$	-0.11	-1.39	-4.25	-8.08	-14.38	-20.33
	(-0.34)	(-1.45)	(-2.58)	(-3.30)	(-4.55)	(-5.12)
R^2	[0.0]	[1.5]	[5.3]	[9.1]	[15.9]	[19.0]

(b) $xr_{t,n} = \gamma_{0,n} + \gamma_{nlp,n} NLP_t + u_{t,n}$

	Maturity (month)					
	2	3	4	5	6	
$\gamma_{0,n}$	0.78	2.91	5.25	8.52	12.32	16.40
	(2.27)	(3.57)	(3.62)	(3.89)	(4.12)	(4.23)
$\gamma_{nlp,n}$	-0.07	1.33	3.88	7.22	11.06	15.55
	(-0.18)	(1.18)	(1.91)	(2.48)	(2.93)	(3.38)
R^2	[0.0]	[1.4]	[4.4]	[7.3]	[9.4]	[11.1]

(c) $xr_{t,n} = \gamma_{0,n} + \gamma_{z,n} z_t + \gamma_{l,n} l_t + \gamma_{nlp,n} NLP_t + u_{t,n}$

	Maturity (month)					
	2	3	4	5	6	
$\gamma_{0,n}$	0.78	2.91	5.25	8.52	12.32	16.40
	(2.33)	(3.66)	(3.83)	(4.24)	(4.71)	(5.04)
$\gamma_{z,n}$	1.08	2.38	5.77	10.12	15.38	22.09
	(2.00)	(2.13)	(3.06)	(3.40)	(3.86)	(4.28)
$\gamma_{l,n}$	0.39	0.17	-0.32	-1.12	-4.10	-5.65
	(0.93)	(0.18)	(-0.21)	(-0.45)	(-1.23)	(-1.25)
$\gamma_{nlp,n}$	0.60	2.54	6.55	11.69	16.96	24.11
	(1.44)	(2.10)	(2.83)	(3.36)	(3.89)	(4.44)
R^2	[1.2]	[4.5]	[12.5]	[19.7]	[28.7]	[34.7]